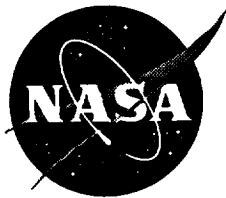


NASA/CR-1998-206955



The Effects of Crossflow On The Pressures and Lift Induced By The Fountain Generated Between Two Impinging Jets

Richard E. Kuhn

*Defense Group, Inc.
16527 Sambroso Place
San Diego, California 92128*

Prepared for
Ames Research Center
CONTRACT NAS2-14384

National Aeronautics and
Space Administration

Ames Research Center
Moffett Field, California 93035-1000

February 1998

TABLE OF CONTENTS

	page
INTRODUCTION	1
SYMBOLS	2
TANDEM JETS	6
Pressure Data	6
Hover Suckdown and Fountain	7
Fountain	7
Suckdown	9
Out-of-Ground-Effect Lift Loss	10
Wake Truncation	12
Ground Vortex	13
Ground Vortex Positive Lift	13
Ground Vortex Negative Lift	13
Upper Surface Lift	14
Effect of Crossflow	15
Fountain lift	15
Suckdown	15
Comparison with Experimental Data	16
SIDE-BY-SIDE JETS	17
Pressure Data	17
Lift Increments	17
Comparison with Experimental Data	19
CONCLUDING REMARKS	20
REFERENCES	21

THE EFFECTS OF CROSSFLOW ON THE PRESSURES AND LIFT INDUCED BY THE FOUNTAIN GENERATED BETWEEN TWO IMPINGING JETS

By

Richard E Kuhn

INTRODUCTION

When a jet or fan powered STOVL aircraft is hovering, or in transition between hover and conventional flight, the lifting jet streams induce suction pressures on the lower surface that cause a lift loss and, generally, a nose up pitching moment. Sketches of the flow fields involved are presented in figure 1. These flow fields and the forces and moments they induce have been studied in many investigations, such as those summarized in references 1-6.

In hover out of ground effect (upper left in figure 1), the entrainment action of the downward directed jets induced suction pressures on the lower surface causing a small lift loss. Close to the ground, (upper right in figure 1) the wall jets flowing radially outward from the point at which the jets impinge greatly increase the entrainment area and the resulting lift loss or suckdown. A fountain flow is generated where the wall jets from multiple jet configurations meet. The impingement of this fountain flow on the configuration partially offsets the suckdown induced by the wall jets. Early methods for estimating the net suckdown are presented in references 7 and 8. These methods were extended to include estimation of the pitching moments in reference 9.

In transition out of ground effect (lower left in figure 1) the jet streams are swept rearward by the interaction with the free stream and roll up into vortex pairs. These vortices, and to a lesser extent the blockage and viscous entrainment action of the jet(s) induce suction pressures on the lower surface of the aircraft, generally causing a loss in lift and a nose up pitching moment. The path that the jets take and the pressures and forces induced are summarized in references 2 - 4 and the development of empirical methods for estimating the aerodynamic effects induced are presented in references 6, 7, 10 and 11.

In ground effect at transition speeds (STOL operation) all the above flow phenomena are present, but modified by the proximity of the ground. In addition a ground vortex is formed by the action of the free stream in opposing the wall jet flowing forward from the impingement point of the front jet(s) (lower right in figure 1). Studies of the ground vortex and methods for estimating its effects are presented in references 5, 6, 10, 12, 13, 14 and 15.

Reference 15 analyzed the detailed pressure data from reference 14 for the single jet case and presented a method for including the effects of the ground vortex in the induced lift estimates. The present study extends the work of reference 15 to two jet configurations and the effect of crossflow on the contribution of the fountain generated between tandem and side-by-side jets.

SYMBOLS

A	Aspect ratio of planform or element of configuration under consideration	
A_j	Jet exit area, total area unless otherwise noted	sq. ft.
A_{aft}	Planform area aft of rear jet	sq. ft.
$A_{GV,neg}$	Planform area between zero pressure line and front jet	sq. ft.
$A_{GV,pos}$	Planform area forward of zero pressure line	sq. ft.
C_{L_w}	Power off lift curve slope	
C_p	Pressure coefficient $C_p = \Delta P / q_j$	
$C_{p,g}$	Pressure coefficient on the ground	
d	Diameter of individual jet(s)	ft.
D_e	Equivalent diameter of total jet area	ft.
D_p	Equivalent diameter of planform area	ft.
e	Half distance between jets	ft.
f_p	Planform fineness ratio	
h	Height above ground	ft.
h_f	Height of break in fountain lift curve	ft.

H_s	Height parameter used in hover suckdown calculation (eq. 20)	
h_{tv}	Height below which trapped vortex condition occurs in hover (eq. 58)	
K_{cf}	Ratio of crossflow lift to hover suckdown (eq. 55 & 63)	
$K_{L,A}$	Factor used to account for aspect ratio on jet induced lift loss (eq. 28-29)	
$K_{L,I}$	Factor used to account for effect of jet position on jet induced lift loss (eq. 30)	
$K_{L,I}$	Factor used to account for mutual interference between side-by-side jets (eq. 61)	
K_A	Factor used to account for tandem jet effect on jet induced lift loss (eq. 31)	
$K_{T,x}$	Factor used to account for jet position on jet flap effect (eq. 33)	
$K_{T,b}$	Factor used to account for jet span on jet flap effect (eq. 34-35)	
$K_{s,high}$	Factor used in calculating hover suckdown at higher heights (eq. 22)	
$K_{s,inb}$	Factor used in calculating hover suckdown on areas inboard of the jets (eq. 21)	
$K_{s,out}$	Factor used in calculating hover suckdown on areas outboard of the jets (eq. 23)	
K'_{tv}	Adjustment factor for effect of 'trapped vortex' in hover (eq. 56 and 57)	
K_{tgv}	Adjustment factor for effect of trapping of the ground vortex at low heights (eq. 50)	
L	Lift	lb.
ΔL	Lift increment	lb.
NPR	Nozzle Pressure Ratio, $NPR = 2.0$	
ΔP	Increment of pressure induced by ground proximity	lb./ft ²
per	Total perimeter of jets	ft.
q	Free stream dynamic pressure	lb./ft ²
q_j	Jet dynamic pressure, $q_j = T/2A_j$	lb./ft ²

S	Total planform area of configuration, or part of configuration under consideration	sq. ft.
S _{aft}	Planform area aft of the jet	sq. ft.
S _{fwd}	Planform area forward of the jet	sq. ft.
S _{ref}	Reference area used in calculation of coefficients	sq. ft.
S _I	Area of sections 1, 2, 3 or 4 used in calculating hover suckdown (see eq. 15)	sq. ft.
T	Total jet thrust	lb.
V _e	Effective velocity ratio. $V_e = \sqrt{q/q_j}$	
x	Longitudinal distance ahead of jet station	ft.
X ₀	Half width of fountain in x direction (eq. 5-6)	ft.
X'	Longitudinal distance, on model centerline, of zero pressure point ahead of jet (eq. 40)	ft.
X' _{mac}	Longitudinal distance of zero pressure line ahead of jet at lateral station of MAC (eq. 47)	ft.
X''	Distance from center of ground vortex to wing leading edge at spanwise position of mean aerodynamic chord (eq. 46)	ft.
X _{s,out}	Distance from jet to center of area aft of rear jet	ft.
X _{jet}	Station at which jet is located	ft.
X _{L.E.}	Station at which leading edge of MAC is located	ft.
Y	Half width of planform at point midway between jets	ft.
Y _j	Width of planform at jet location	ft.
Y _{ave}	Average width of planform ahead of jet station	ft.
y	Lateral distance from centerline	ft.
Y _{mac}	Lateral distance of MAC from centerline	ft.
$\Delta\alpha_{us}$	Upwash angle induced by ground vortex. (eq. 48 and 49)	deg.

SUBSCRIPTS

aft	Aft jet, or aft of jet
cf	Crossflow term
data	Experimental data
est	Estimate
fwd	Forward jet, or forward of the jet
f	Fountain
f,h	Fountain estimate in hover
GV,p	Positive ground vortex contribution
GV,n	Negative ground vortex contribution
h	Hover
high	at the higher heights, (eq. 17)
inb	Inboard, between jet and fountain, (eq. 16)
j	Jet
jf	Jet flap effect
out	Outboard of jet, (eq. 18)
neg	Negative pressure region
mac	Mean aerodynamic chord
pos	Positive pressure region
s,h	Suckdown estimate in hover
tv	Trapped vortex condition
us	Upper surface contribution
w	Jet wake contribution
w,t	Truncation of jet wake

EXPONENTS

b	Exponent used in estimating fountain width (eq. 7)
f	Exponent used in fountain pressure estimate (eq. 10 & 11)
g & i	Exponents used in hover suckdown estimates (eq. 24 & 25)

TANDEM JETS

PRESSURE DATA

Data for three tandem jet configurations with 12, 8, and 4 inch jet spacings ($e/d = 5, 3.33$ and 1.67 respectively) are available in reference 14. The model used in reference 14 (fig. 2) was a simple flat plate configuration with replaceable centerline plates to facilitate providing various jet locations and spacings. The jet configurations used in this analysis are defined below.

Configuration	e/d	Jet Station		Jet dia. in.	Ref. station in.
		front	rear		
I	3.33	12	20	1.2	16
II	5	12	24	1.2	18
V	1.67	20	24	1.2	22
side-by-side	1.48	12	--	.85	12

The jets were simple convergent jets with moderate contraction ratio and perforated plates upstream of the nozzle to provide smooth exit flow. The data available from reference 14, and the analysis presented here, are limited to circular vertical jets.

Unfortunately during the investigation reported in reference 14 it was found that the impingement of the jets on endless-belt moving-ground board caused the belt to distort and the tests had to be made over a fixed ground board. Reference 15 shows a considerable effect of moving over the ground on the ground vortex position and on the pressures and lift induced by a single impinging jet. There are probably related effects on the fountain and pressures induced between jets but there is no data available to evaluate these effects.

A sketch of the pressures induced ahead of the jet, on the model and on the ground, by the ground vortex is shown in figure 3a. An overview of the pressures induced by the three tandem jet configurations analyzed here is given by the centerline pressure distributions shown in figure 4. At the lowest heights the positive pressures induced by the impingement of the fountain, and the added suckdown pressures induced ahead of and aft of the fountain (between the fountain and the jets) are clearly shown between the jets. Also the ground vortex induced positive pressure ahead of, and the negative pressures induced in the region of, the ground vortex are shown at the lowest heights ahead of the front jet. At the higher heights the negative pressures induced in the wake of the rear jet predominate; and these are increased by the suckdown pressures induced at low heights.

The effect of height and velocity ratio on the location and spanwise distribution of the fountain and ground vortex induced

pressures are illustrated in figures 5, 6, and 7. Comparison of the estimated location of the zero pressure line (the line between the positive pressures forward, and the negative pressures induced by the ground vortex) is in good agreement with the experimental data. These estimates were made on the basis of the front jet operating alone.

Analysis of all the data available from the three jet spacings shows that the predominant factors in determining the net lift loss are the suckdown induced when hovering in ground effect and the jet wake lift loss induced out of ground effect. These two increments, and the other factors that add up to the net induced lift loss, are shown schematically in figure 8. The net lift loss can be expressed as;

$$\frac{L}{T} = \left(\frac{\Delta L}{T}\right)_{s,h} + \left(\frac{\Delta L}{T}\right)_w + \left(\frac{\Delta L}{T}\right)_{w,t} + \left(\frac{\Delta L}{T}\right)_{gv,p} + \left(\frac{\Delta L}{T}\right)_{gv,r} + \left(\frac{\Delta L}{T}\right)_{uw} + \left(\frac{\Delta L}{T}\right)_f + \left(\frac{\Delta L}{T}\right)_{cf} \quad (1)$$

where $\left(\frac{\Delta L}{T}\right)_{s,h}$ is the hover suckdown lift loss (in ground effect) estimated by the method of reference 9, and $\left(\frac{\Delta L}{T}\right)_w$ is the lift loss induced at forward speed out of ground effect (jet wake term) estimated by the method of reference 11. The analysis indicates that the sum of these two increments can generally be thought of as a "worst case" estimate of the lift loss experienced at transition speeds close to the ground. Some of the other terms increase the lift loss but those that reduce the lift loss are larger, resulting in a net reduction from the "worst case" sum of the hover suckdown and the jet wake terms as shown in figure 8. The factors determining all these terms are examined in the following sections. For completeness key expressions from references 9, 11, and 15 for estimating Hover suckdown and fountain, jet wake and ground vortex effects needed in the analysis are included below.

HOVER SUCKDOWN AND FOUNTAIN

For the present flat plate configuration with circular vertical jets the method of reference 9 for estimating the hover fountain lift and suckdown, can be reduced to;

$$\left(\frac{\Delta L}{T}\right)_h = \left(\frac{\Delta L}{T}\right)_{f,h} + \left(\frac{\Delta L}{T}\right)_{s,h} \quad (2)$$

Fountain

The fountain term (from ref. 9) is the average pressure in the

fountain region multiplied by the area and, in hover, is given by;

$$\left(\frac{\Delta L}{T}\right)_{f,h} = C_{p,f} q_j S_f / T \quad (3)$$

where the area is;

$$S_f = 4YX_o \quad (4)$$

and Y is the half width of the planform midway between the jets and X_o is the half width (in the x direction) of the fountain region. For closely spaced jets ($e/d < 1.5$) the fountain positive pressure region extends from jet to jet and;

$$X_o = e \quad (5)$$

For spacing ratios greater than $e/d = 1.5$, and at the lower heights, the half width of the fountain for the present configuration;

$$X_o = e .36 \left(\frac{Y}{d}\right)^{-.08} \left(\frac{h}{e}\right)^b \quad (6)$$

where the exponent b is given by;

$$b = .6 \left(\frac{e}{d}\right)^{-.16} \left(\frac{Y}{d}\right)^{.25} \quad (7)$$

At the higher heights X_o reaches a limit which is taken as;

$$X_o = .5e \quad (8)$$

The average pressure is calculated in two height ranges. At the lower heights the average pressure coefficient is given by;

$$C_{p,f} = .16 \left(\frac{S}{A_j}\right)^{-.72} \left(\frac{e}{d}\right)^{-.5} \left(\frac{Y}{d}\right)^{.25} \left(\frac{h}{e}\right)^f \quad (9)$$

where the exponent f is given by;

$$f = -4 \left(\frac{e}{d}\right)^{.5} \quad \text{for } e/d > 3.3 \quad (10)$$

$$f = -2.2 \quad \text{for } e/d < 3.3 \quad (11)$$

At the higher heights the average pressure falls off at a much more rapid rate because we are basically seeing the effects of the unsteady 'top' of the fountain (ref. 9). The height at which these

effects become apparent is given by;

$$h_f = 3.7 (NPR)^{-0.5} \left(\frac{e}{d}\right)^{-0.2} \quad (12)$$

Above h_f the average fountain pressure is given by;

$$C_{p,f} = .16 \left(\frac{S}{A_j}\right)^{-0.72} \left(\frac{e}{d}\right)^{-0.5} \left(\frac{Y}{d}\right)^{0.25} \left(\frac{h}{e}\right)^f \left(\frac{h_f}{h}\right)^3 \quad (13)$$

Suckdown

The suckdown term $\left(\frac{\Delta L}{T}\right)_{s,h}$ (as presented in ref. 9) is the sum of the suckdown in 4 areas; the area ahead of the front jet (S_1), between the fountain and the front jet (S_2), between the fountain and the rear jet (S_3) and aft of the rear jet (S_4). The hover suckdown is given by;

$$\left(\frac{\Delta L}{T}\right)_{s,h} = \left(\frac{\Delta L_{S,1}}{T} + \frac{\Delta L_{S,2}}{T} + \frac{\Delta L_{S,3}}{T} + \frac{\Delta L_{S,4}}{T}\right) \quad (14)$$

For the present configuration with equal thrust from each of the two jets the suckdown in each of the four regions is given by;

$$\frac{\Delta L_{S,x}}{T} = C_{p,s} Q_j S_x / T \quad (15)$$

where S_i is the area of the region under consideration. For the regions ahead of the front jet and behind the rear jets S_i is the geometric area. For the regions between the jets and the fountain S_i is the difference between the geometric area and half the fountain impingement area S_f .

The average pressure between the jets and the fountain is given by;

$$C_{p,s} = K_{s,low} H_s^g \quad \text{at the lower heights} \quad (16)$$

$$C_{p,s} = K_{s,high} H_s^{-1.8} \quad \text{at the higher heights} \quad (17)$$

Similarly average pressure outboard of the jets is given by;

$$C_{p,s} = K_{s,out} H_s^1 \quad \text{at the lower heights, while} \quad (18)$$

$$C_{p,s} = K_{s,high} H_s^{-1.8} \quad \text{at the higher heights} \quad (19)$$

where the height parameter H_s is given by;

$$H_s = \frac{h}{D_p - D_e} NPR^{.8/(Y/d)} \quad (20)$$

and

$$K_{s,low} = -.3 \left(\frac{S}{A_j} \right)^{-1} \left(\frac{e}{d} \right)^{-.15} \quad (21)$$

$$K_{s,high} = -.135 \left(\frac{S}{A_j} \right)^{-1} \left(\frac{e}{d} \right)^{.5} \left(\frac{Y_j}{d} \right)^{-.36} \quad (22)$$

$$K_{s,out} = -.062 \left(\frac{S}{A_j} \right)^{-.84} \left(\frac{Y_j}{d} \right)^{.25} \left(\frac{X_{s,out}}{d} \right)^{-.5} \quad (23)$$

The exponents used above are given by;

$$g = -.38 \left(\frac{S}{A_j} \right)^{.36} \left(\frac{e}{d} \right)^{-.25} \left(\frac{Y_j}{d} \right)^{-.15} \quad (24)$$

$$i = -.96 \left(\frac{e}{d} \right)^{-.25} \left(\frac{X_{s,out}}{d} \right)^{.38} \quad (25)$$

The above expressions calculate two values of suckdown at each height. The change over height is not given. The larger (less negative) value is used.

OUT-OF-GROUND-EFFECT LIFT LOSS

In transition the free stream deflects the jets aft and causes them to generate vortex pairs in their wake. The jet induced effects due to this wake flow field can be estimated by the method of reference 11. For each jet there are two components to the estimate; a lift loss induced by the jet/free-stream interaction and a lift gain due to a 'jet-flap' type effect which partially offsets the jet induced lift loss. There is also a lift loss increment that occurs in hover out of ground effect. With a two jet configuration there are

therefore five parts to the lift estimate;

$$\left(\frac{\Delta L}{T}\right)_v = \left(\frac{\Delta L}{T}\right)_{j, fwd} + \left(\frac{\Delta L}{T}\right)_{jf, fwd} + \left(\frac{\Delta L}{T}\right)_{j, aft} + \left(\frac{\Delta L}{T}\right)_{jf, aft} + \left(\frac{\Delta L}{T}\right)_{v_e=0} \quad (26)$$

where $\left(\frac{\Delta L}{T}\right)_{v_e=0}$ is the hover lift loss (from ref. 9) out of ground effect;

$$\left(\frac{\Delta L}{T}\right)_{v_e=0} = -.0001\sqrt{S/A_j} (per/d)^{1.58} (NPR)^{-.5} \quad (27)$$

The jet induced lift loss in transition for the current twin-jet flat-plate configuration is (from ref. 11) given by;

$$\left(\frac{\Delta L}{T}\right)_{j, fwd} = \left[-10 V_e^{2.4} (S/A_{j, fwd})^{-.08} + 2 \left(\frac{S}{A_{j, fwd}}\right)^{.18} V_e^3 \right] K_{L,A} K_{L,X} K_m \quad (28)$$

where

$$K_{L,A} = A^{-.4} \quad \text{for } A < 1 \quad (29)$$

$$K_{L,A} = 1 \quad \text{for } A > 1 \quad (30)$$

$$K_{L,X} = 1.4 - .8 (S_{fwd}/S) - (1 - S_{fwd}/S)^{15} \quad (31)$$

$$K_m = 1 + .005 \frac{S_{fwd}}{A_{j, fwd}} \frac{2e}{d_{fwd}} \quad (32)$$

The 'jet flap' effect lift gain for the current twin-jet flat-plate configuration is given by;

$$\left(\frac{\Delta L}{T}\right)_{jf, fwd} = \left[30 V_e^2 \left(\frac{S}{A_{j, fwd}}\right)^{.5} \frac{A}{A+2} \right] K_{T,x} K_{T,b} \quad (33)$$

where

$$K_{T,x} = .7 + .3 \left(\frac{S_{fwd}}{S}\right) - .7 \left(1 - \frac{S_{fwd}}{S}\right)^{15} \quad (34)$$

and

$$K_{T,b} = \frac{b_j}{b} A \quad \text{for } A < 1 \quad (35)$$

$$K_{T,b} = \frac{b_j}{b} \quad \text{for } A > 1 \quad (36)$$

With tandem jet configurations the rear jet is operating in the wake of the front jet and therefore operating at a lower effective velocity ratio. The effective velocity ratio at the rear jet is given by;

$$V_{e, aft} = V_e \frac{(2e/d_{fwd}) - 1}{(2e/d_{fwd}) + .75} \quad (37)$$

The jet induced lift loss and the 'jet flap' type lift gain are therefore calculated at this effective velocity ratio;

$$\left(\frac{\Delta L}{T}\right)_{j, aft} = \left[-10 V_{e, aft}^{2.4} (S/A_{j, aft})^{-.08} + 2 \left(\frac{S}{A_{j, aft}}\right)^{.18} V_{e, aft}^3 \right] K_{L,A} K_{L,x} \quad (38)$$

and

$$\left(\frac{\Delta L}{T}\right)_{jf, aft} = \left[30 V_{e, aft}^2 \left(\frac{S}{A_{j, aft}}\right)^{.5} \frac{A}{A+2} \right] K_{T,x} K_{T,b} \quad (39)$$

It must be noted that the above expressions (eq. 27-39) contain only those factors from ref. 9 and 11 necessary to estimate the induced effects on the present flat-plate tandem-jet configurations. For other configurations resort must be made to references 9 and 11.

Wake Truncation

Reference 15 shows that the out-of-ground-effect lift loss due the wake term $\left(\frac{\Delta L}{T}\right)_w$ is reduced due to the truncation of the wake as the configuration nears the ground (fig. 1). In the present analysis the term used to account for this truncation is taken from reference 15, using the diameter of the rear jet;

$$\left(\frac{\Delta L}{T}\right)_{w,t} = .05 V_e \left(\frac{h}{d}\right)^{-1.5} q_j S_{aft} / T \quad (40)$$

GROUND VORTEX

Ground Vortex Positive Lift

Positive pressures are induced forward on the configuration (fig. 5) by the action of the ground vortex in forcing the free stream to flow up and over the vortex (fig. 3). The zero pressure line between these positive pressures and the negative pressures induced by the ground vortex appears to be established by the front jet alone (fig. 5). As presented in reference 15, the location of the zero pressure point on the model centerline for this model with vertical jets tested over a fixed ground board is given by;

$$\frac{X'}{d_{fwd}} = .6 \left(\frac{S}{A_{j, fwd}} \right)^{.2} V_o^{-.4} \left(\frac{h}{d} \right)^{.06 V_o^{-.7}} \quad (41)$$

The zero pressure line is parabolic in shape and is given by;

$$y = 2\sqrt{X'(X'-x)} \quad (42)$$

As shown in figure 9, integration of the pressures forward of the zero pressure line produces lift increments in reasonable agreement with those estimated by the method of reference 15 based on the diameter of the front jet. For the present analysis, therefore $\left(\frac{\Delta L}{T} \right)_{GV, P}$ is estimated by the method of reference 15 using the front jet diameter;

$$\left(\frac{\Delta L}{T} \right)_{GV, P} = .46 V_o f_p^{.5} \left(\frac{h}{d} \right)^{-1} \left(\frac{S_{fwd}}{A_j} \right)^{-.4} \frac{Q_j A_{GV, P}}{T} \quad (43)$$

Ground Vortex Negative Lift

The negative lift induced by the ground vortex are shown in figure 10 by the increased lift loss (increased relative to the sum of the hover suckdown and the out-of-ground-effect lift loss) induced forward of the front jet. Unfortunately there is no easy way to separate the ground induced suckdown from the other factors involved at forward speeds. For the present analysis the factor representing the ground vortex induced suckdown forward of the front jet, $\left(\frac{\Delta L}{T} \right)_{GV, N}$, is estimated by the method of reference 15, based on the front jet diameter, using the less negative of the two following expressions.

At the lower heights;

$$\left(\frac{\Delta L}{T} \right)_{GV, N} = -10 V_o \left(\frac{Y_{ave}}{d_{fwd}} \right)^{-2} \left(\frac{h}{d_{fwd}} \right)^{-8.4 / \sqrt{S_{fwd}/A_{j, fwd}}} \frac{Q_j A_{GV, N}}{T} \quad (44)$$

At the higher heights;

$$\left(\frac{\Delta L}{T}\right)_{GV,n} = -.1 f_p^{.25} \left(\frac{h}{d_{fwd}}\right)^{-2} \frac{Q_j A_{GV,n}}{T} \quad (45)$$

Upper Surface Lift

As indicated in reference 15 the blockage effect of the ground vortex forces the free stream to flow up and over it (fig. 3) placing the configuration in an upflow. The method of ref. 15 assumes the lift generated is equivalent to operating at an effective angle of attack;

$$\left(\frac{\Delta L}{T}\right)_{us} = C_{L\alpha} \Delta\alpha_{us} Q_j V_o^2 S_{ref} / T \quad (46)$$

The effective angle of attack depends on the location of the ground vortex center relative to the leading edge of the planform MAC (Mean Aerodynamic Chord) as determined by X'' ;

$$X'' = \frac{X'_{mac}}{2} - (X_{jet} - X_{L.E.}) \quad (47)$$

where

$$X'_{mac} = X' - \frac{Y_{mac}^2}{4X'} \quad (48)$$

for negative values of X''

$$\Delta\alpha_{us} = \left[.7 - .7 \frac{X''}{d} - .35 \left| \frac{X''}{d} \right|^{1.2} \right] \frac{K_{tgv}}{V_o h/d} \quad (49)$$

for positive values of X''

$$\Delta\alpha_{us} = \left[.7 - .7 \frac{X''}{d} + .16 \left(\frac{X''}{d} \right)^{1.5} \right] \frac{K_{tgv}}{V_o h/d} \quad (50)$$

and K_{tgv} accounts for the effects of 'trapping' the ground vortex under the configuration at low heights (fig. 3).

Below $h = .5 \sqrt{S/A_j} V_o X'_{mac}$

$$K_{tgv} = \frac{h}{.5 \sqrt{S/A_j} V_o X'_{mac}} \quad (51)$$

$$\text{Above } h = .5 \sqrt{S/A_j} V_o X'_{mac}$$

$$K_{tgv} = 1.0$$

(52)

EFFECT OF CROSSFLOW

Fountain Lift

The effect of the crossflow on the fountain term $\left(\frac{\Delta L}{T}\right)_f$ (fig. 11) and was derived by integrating the positive pressure induced in the fountain impingement area (see fig. 5) at each height and velocity ratio. At a given height the lift was found to decrease with increasing crossflow velocity. The ratio of the lift increment with crossflow, to that determined in hover ($V_e = 0$) is presented in figure 11. For the present analysis the fountain lift in a crossflow can be taken as;

$$\left(\frac{\Delta L}{T}\right)_f = \left(\frac{\Delta L}{T}\right)_{f,h} \left[1 - 0.6 \left(\frac{h}{d'}\right)^{2.5} \right] V_o \quad (53)$$

where $\left(\frac{\Delta L}{T}\right)_{f,h}$ is determined by eq. 3 and d' is the individual diameter of each jet in a tandem pair and the equivalent diameter of a side-by-side pair.

Suckdown

The effects of the crossflow on the lift induced in each of the four lower surface areas (obtained by integration of pressures in each area) are shown in figure 10 for configuration I. As noted above, the lift induced out of ground effect ($h/D_e = 25$, and the lift loss induced in hover ($V_e = 0$), are responsible for most of the lift loss. The effect of the ground vortex in increasing the lift loss on the forward area (S_1) at the lower heights is shown and discussed above. However over most of the other areas the crossflow decreases the lift loss (particularly between the front jet and the fountain (S_7)).

A way of developing methods for estimating the lift loss in each area did not appear practical. Instead the effect of the crossflow on the combined suckdown was found by subtracting the sum of the other terms, developed in the previous sections, from the experimental data;

$$\left(\frac{\Delta L}{T}\right)_{cf} = \left(\frac{\Delta L}{T}\right)_{exp} - \left[\left(\frac{\Delta L}{T}\right)_{s,h} + \left(\frac{\Delta L}{T}\right)_w + \left(\frac{\Delta L}{T}\right)_{w,t} + \left(\frac{\Delta L}{T}\right)_{gv,p} + \left(\frac{\Delta L}{T}\right)_{gv,n} + \left(\frac{\Delta L}{T}\right)_{us} + \left(\frac{\Delta L}{T}\right)_f \right]$$

The resulting crossflow increment was found to be proportional to the crossflow velocity ratio V_e as shown in figure 12a which presents the ratio of the crossflow increment to the hover suckdown term. This ratio, K_{cf} , is a function of height and jet spacing and decreases rapidly at heights below which the hovering trapped vortex condition (discussed in ref. 9) is encountered. In the present analysis the crossflow lift increment is given by;

$$\left(\frac{\Delta L}{T}\right)_{cf} = K_{cf} \left(\frac{\Delta L}{T}\right)_{s,h} \quad (55)$$

where

$$K_{cf} = K'_{tv} 4.2 V_e \left(\frac{h}{e}\right)^{.5} \quad (56)$$

and

$$K'_{tv} = \frac{h}{h_{tv}} \quad \text{below } h = h_{tv} \quad (57)$$

$$K'_{tv} = 1.0 \quad \text{above } h = h_{tv} \quad (58)$$

and h_{tv} (from ref. 9) is given by;

$$h_{tv} = .2(D_p - D_e) \quad (59)$$

Comparison with Experimental Data

Figure 13 shows that the estimates (eq. 1) are in reasonable agreement with the data on which the expressions are based, except for the configuration with the closest jet spacing at the lowest height. The problem here is in the hover estimates as shown in figure 14. The method of reference 9 significantly over estimates the suckdown for the most closely spaced pair at the lowest heights.

Figure 13 also shows that the simple "worst case" estimate - the sum of the hover suckdown term (eq. 14) and the out-of-ground-effect term (eq. 26) - over estimates the net lift loss at the higher velocity ratios.

SIDE-BY-SIDE JETS

PRESSURE DATA

Data are available for only one side-by-side jet pair, and this configuration is rather closely spaced as shown in figure 2. The two jets were located at station 12 and each had a diameter of .85 inches. Typical chordwise pressure distributions are shown in figure 15. The positive pressures generated by the fountain between this closely spaced pair of jets is observed only on the centerline at the lowest heights.

The effects of the ground vortex are most clearly apparent (fig. 15) in the positive pressures generated forward of the vortex. Figure 15 also shows that the point at which the pressures go to zero is further aft on the centerline than at the next outboard station ($y = 1.5$ in.)

The location and shape of the zero pressure line for the side-by-side pair is compared with that for the equivalent single jet in figure 16. The estimates of the zero pressure line shape and location, presented in figure 16, were made assuming that each jet is operating independently; that is, the estimate is made (using eq. 40 and 41) for each jet alone based on its diameter, area and height diameter ratio.

Although there is considerable scatter in both the single jet and jet pair data the zero pressure line for the pair appears to be even further aft than the estimate indicates. A similar finding was reported in reference 16 where the zero pressure point (on the ground rather than on the lower surface of the configuration as in the present study) was found to be further aft for the side-by-side pair than for one of the pair operating alone.

The positive lift increment generated by the ground vortex was obtained by integrating these positive pressures forward of the zero pressure line and compared with estimates made by equation 42 in figure 17. The method tends to underestimate the lift increment induced at the lowest heights and higher velocity ratios.

LIFT INCREMENTS

The lift increments for the side-by-side pair were examined in the same manner used for the tandem jets. The net lift is given by the sum of the increments;

$$\frac{L}{T} = \left(\frac{\Delta L}{T}\right)_{s,h} + \left(\frac{\Delta L}{T}\right)_w + \left(\frac{\Delta L}{T}\right)_{w,t} + \left(\frac{\Delta L}{T}\right)_{GV,P} + \left(\frac{\Delta L}{T}\right)_{GV,R} + \left(\frac{\Delta L}{T}\right)_{us} + \left(\frac{\Delta L}{T}\right)_f + \left(\frac{\Delta L}{T}\right)_{cf} \quad (60)$$

where $\left(\frac{\Delta L}{T}\right)_{s,h}$ is the hover suckdown part of the lift loss estimate by the method of reference 9 using eq. 14 above, and $\left(\frac{\Delta L}{T}\right)_v$ is the lift loss induced at forward speed out of ground effect. This increment is estimated by the method of reference 11 using eq. 26, 28 and 33 above with an additional factor added to account for the mutual interference between closely spaced jets. Equation 28 is augmented to read;

$$\left(\frac{\Delta L}{T}\right)_{j, fwd} = \left[-10 V_e^{2.4 (S/A_{j, fwd})^{-0.09}} + 2 \left(\frac{S}{A_{j, fwd}}\right)^{.18} V_e^3 \right] K_{L,x} K_{L,y} K_z K_{L,y} \quad (61)$$

where

$$K_{L,y} = 1.2 - .1 \left(\frac{2e}{d} - 1\right) \quad (62)$$

The fountain lift increment $\left(\frac{\Delta L}{T}\right)_f$ induced by the side-by-side pair decreases with increasing crossflow velocity at about the same rate as that for the tandem jets (fig. 11). Equation 53 is therefore applicable; where d' is the equivalent diameter of the side-by-side pair.

The ground vortex increments $\left(\frac{\Delta L}{T}\right)_{gv,p}$ and $\left(\frac{\Delta L}{T}\right)_{gv,n}$ are each the sum of the increments estimated for each of the jets in the pair based on their individual diameters, areas and height diameter ratios using eq. 43 - 45.

The upper surface increment $\left(\frac{\Delta L}{T}\right)_{us}$ is based on the front jet and is estimated using eq. 46.

The wake truncation increment $\left(\frac{\Delta L}{T}\right)_{w,t}$ is, like the ground vortex terms, the sum of the increments calculated for each jet based on their individual diameter and area using eq. 40.

The crossflow increment $\left(\frac{\Delta L}{T}\right)_{cf}$ was found, as it was for the tandem jets by subtracting the sum of the above increments from the experimental data;

$$\left(\frac{\Delta L}{T}\right)_{cf} = \left(\frac{\Delta L}{T}\right)_{exp} - \left[\left(\frac{\Delta L}{T}\right)_{s,h} + \left(\frac{\Delta L}{T}\right)_v + \left(\frac{\Delta L}{T}\right)_{w,t} + \left(\frac{\Delta L}{T}\right)_{gv,p} + \left(\frac{\Delta L}{T}\right)_{gv,n} + \left(\frac{\Delta L}{T}\right)_{us} + \left(\frac{\Delta L}{T}\right)_f \right]$$

The resulting crossflow increment was found to increase with both h/d and V_e at low V_e 's, but to reach a maximum between $V_e = .10$ and $.15$ and decrease at higher crossflow velocities. Although there is considerable scatter in the data the ratio of the crossflow increment to the hover suckdown increment, K_{cf} , (fig. 18) appears to be given by;

$$K_{cf} = (2V_e - 300V_e^4) \frac{h}{d} K'_{tv} \quad (64)$$

The decrease in K_{cf} at the higher V_e 's for this side-by-side pair is in contrast to the linear variation of K_{cf} with V_e found for the tandem pairs (fig. 12 and eq. 56). It should be noted that the side-by-side pair data was carried to higher values of V_e than the data for the tandem pairs and, had the later been carried to higher V_e 's, they may have also reached a maximum.

COMPARISON WITH EXPERIMENTAL DATA

Figure 19 shows that the estimates (eq. 59) are in reasonable agreement with the data on which the estimating method is based except at the lowest heights. The problem here is in the hover estimates as shown in figure 20 as it was for the closely spaced tandem pair. The method of reference 9 significantly over estimates the suckdown for closely spaced pairs at the lowest heights.

Figure 19 also shows that the simple "worst case" estimate of the sum of the hover suckdown term and the out-of-ground-effect term over estimates the net lift loss at the higher velocity ratios.

CONCLUDING REMARKS

In transition while in ground effect (STOL operation) the suckdown and fountain effects experienced in hover and the jet wake effects induced in transition out of ground effect are still present but modified by ground proximity. In addition a ground vortex is generated ahead of the forward jet(s) that induced both suckdown and lifting pressures on the configuration.

The results of this analysis of data from twin jet configurations indicate that the suckdown induced in hover, and the jet wake effects induced out of ground effect are the primary contributors to the net lift loss in STOL operation.

The analysis also indicates that the direct lift due to the impingement of the fountain generated between two jets is reduced by the crossflow. Fortunately the additional suckdown induced between the fountain and the jets is also reduced. This reduction plus the net effect of the ground vortex results in a net reduction in the lift loss relative to the simple summation of the hover suckdown and the out-of-ground-effect lift loss.

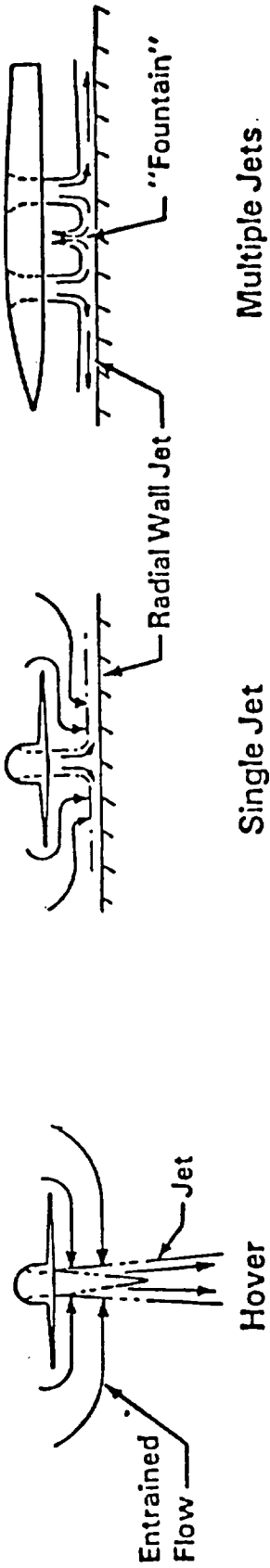
The expressions developed here for estimating elements of the lift loss should be used with caution for several reasons. The data were taken over a fixed ground board. The effects of movement over the ground (the effect of the scrubbing action of the ground on the wall jet generated by the impinging jet) are not known. The data and analysis are also limited to low pressure, circular jets exiting vertically from a simple flat plate configuration.

REFERENCES

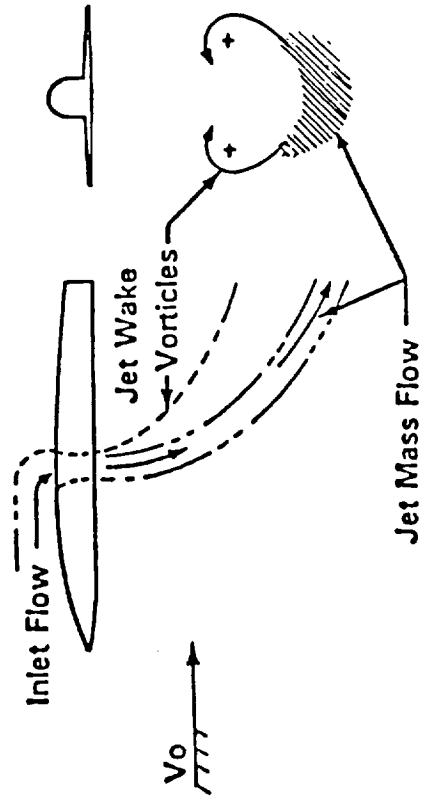
1. Kotansky D.R.; "Jet Flowfields" in "Special Course on V/STOL Aerodynamics," AGARD-R-710, pp 7-1 to 7-48, April 1984.
2. Margason, R.J.; "Fifty Years of Jet in Cross Flow Research." Presented at 72nd AGARD Fluid Dynamics Panel Meeting and Symposium on Computational and Experimental Assessment of Jet in Cross Flow. April, 1993.
3. Margason, R.J.; "Propulsion-Induced Effects Caused by Out-of-Ground Effects," SAE 872307, in "Proceedings of the International Powered Lift Conference," SAE P-203, Dec. 1987, pp 31-58.
4. Anon.; "Analysis of a jet in a Subsonic Crosswind," NASA SP-218, Sept. 1969.
5. Margason, R.J.; "1987 Ground Vortex Workshop" NASA CP-10008, April 1987.
6. Stewart, V.R. and Kuhn, R.E.; "A Method for Estimating the Propulsion Induced Aerodynamic Characteristics of STOL Aircraft in Ground Effect," NADC 80226-60, Aug. 1983.
7. Henderson, C., Clark, J, and Walters, M,; "V/STOL Aerodynamics and Stability and Control Manual," NADC-80017-60, Jan. 1980.
8. Kuhn, R.E.; "An Engineering Method for Estimating the Induced Lift on V/STOL Aircraft Hovering in and out of Ground Effect" NADC Rept. No. NADC-80246-60, Jan. 1981.
9. Kuhn, R.E., Stewart, V.R. and Wardwell, D.A.; "Estimation of Lift and Pitching Moment Induced on Jet STOVL Aircraft Hovering in Ground Effect" WL-TR-93-3046. Aug. 1993.
10. Stewart, V.R. and Kuhn, R.E.; "A Method for Prediction of the Aerodynamic Stability and Control Parameters of STOL Aircraft Configurations - Volume II: STOL Aerodynamic Stability and Control Parameter Estimation Methods" AFWAL-TR-87-3019, June 1987.
11. Kuhn, R.E.; "An Empirical Method for Estimating the Jet Induced Lift and Pitching Moment on STOVL Aircraft out of Ground Effect" WL-TR-96-3042, Jan. 1996.
12. Stewart, V.R. and Kuhn. R.E.; "Lift and Pitching moment induced on Jet STOVL Aircraft by the Ground Vortex - Data Report" WL-TR-93-3045, June 1993.
13. Stewart, V.R. and Kuhn, R.E.; "Estimation of Lift and Pitching Moment Induced on Jet STOVL Aircraft by the Ground Vortex" WL-TR-93-3061, Aug. 1993.

14. Kuhn, R.E. and Stewart, V.R.; "Lift and Pitching Moment Induced on Jet STOVL Aircraft Hovering in Ground Effect - Data Report" WL-TR-93-3044. June 1993.
15. Kuhn, R.E.; "An Analysis of the Pressures, Forces and Moments induced by the Ground Vortex Generated by a Single Impinging Jet" NASA CR-4765, Feb. 1997
16. Barata, Jorge M.M.; "Ground Vortex Formation with Twin Impinging Jets" SAE 962257 In SAE P-306 "International Powered Lift Conference Proceedings" March 1997

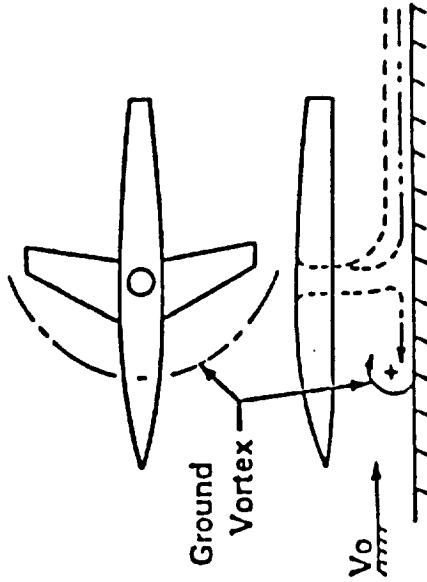
BASIC FLOW FIELDS



Out-of-Ground-Effect



Transition Out-of-Ground-Effect



Transition In-Ground-Effect (STOL Operation)

Figure 1.- Basic flow fields in and out of ground effect.

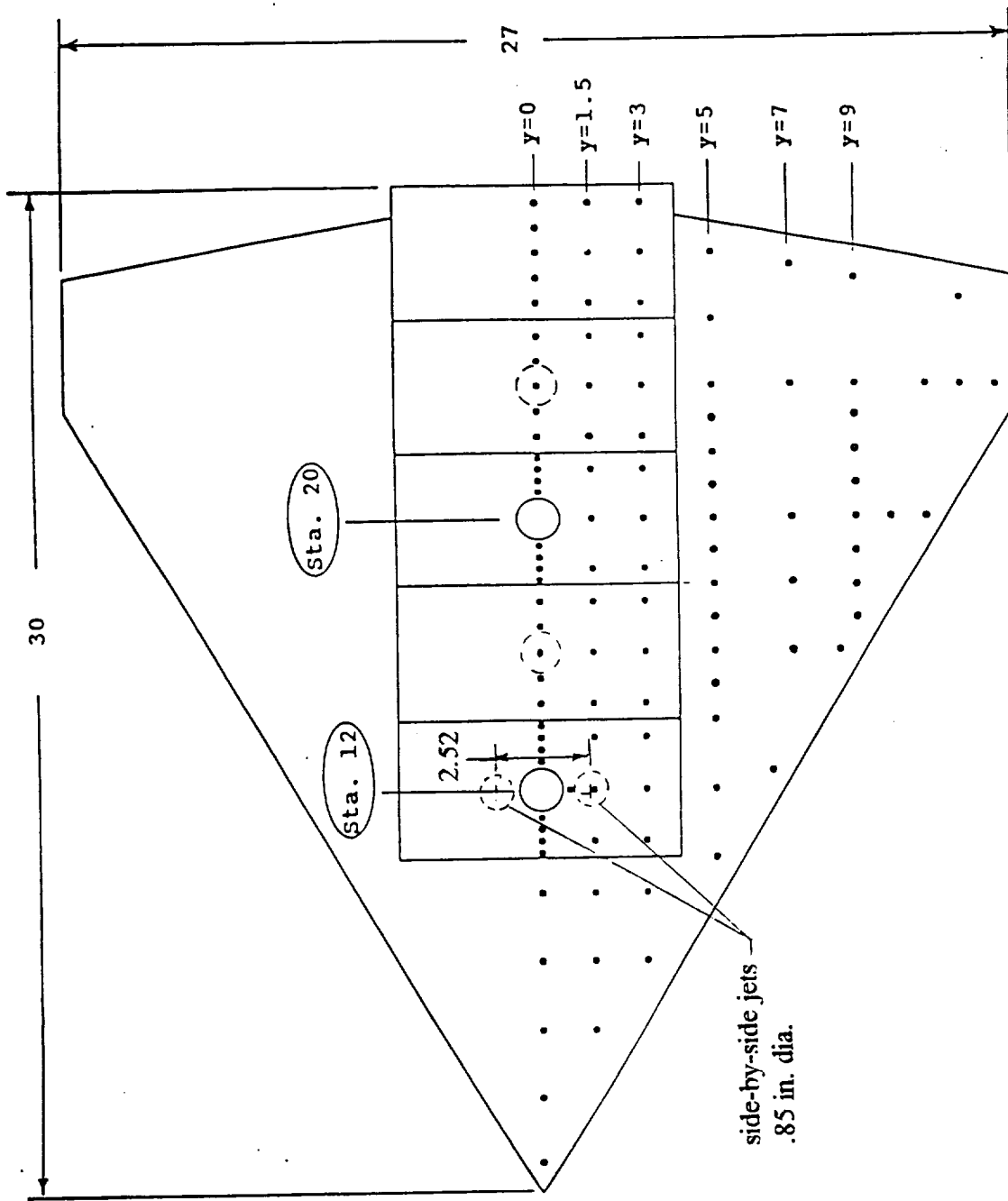
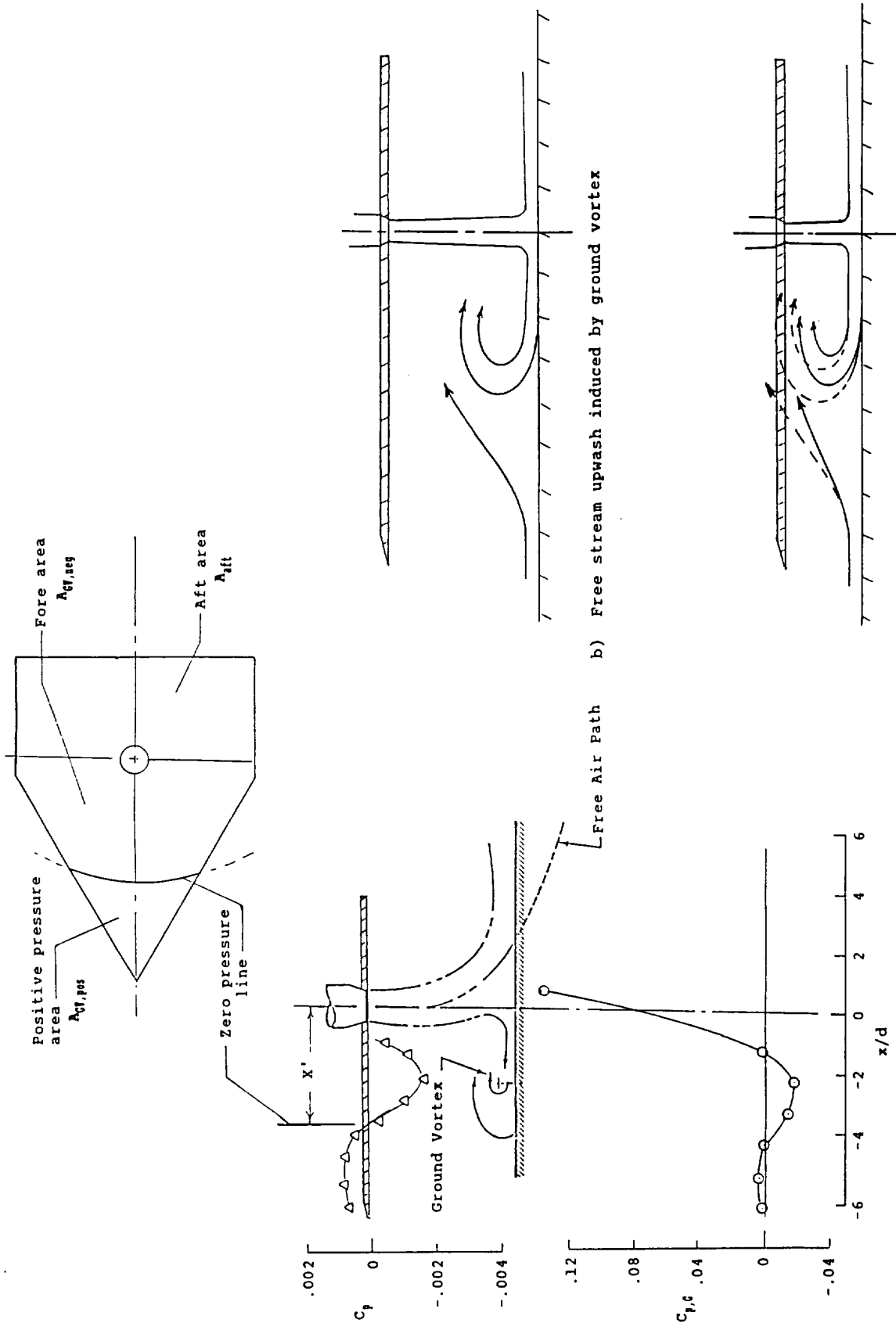


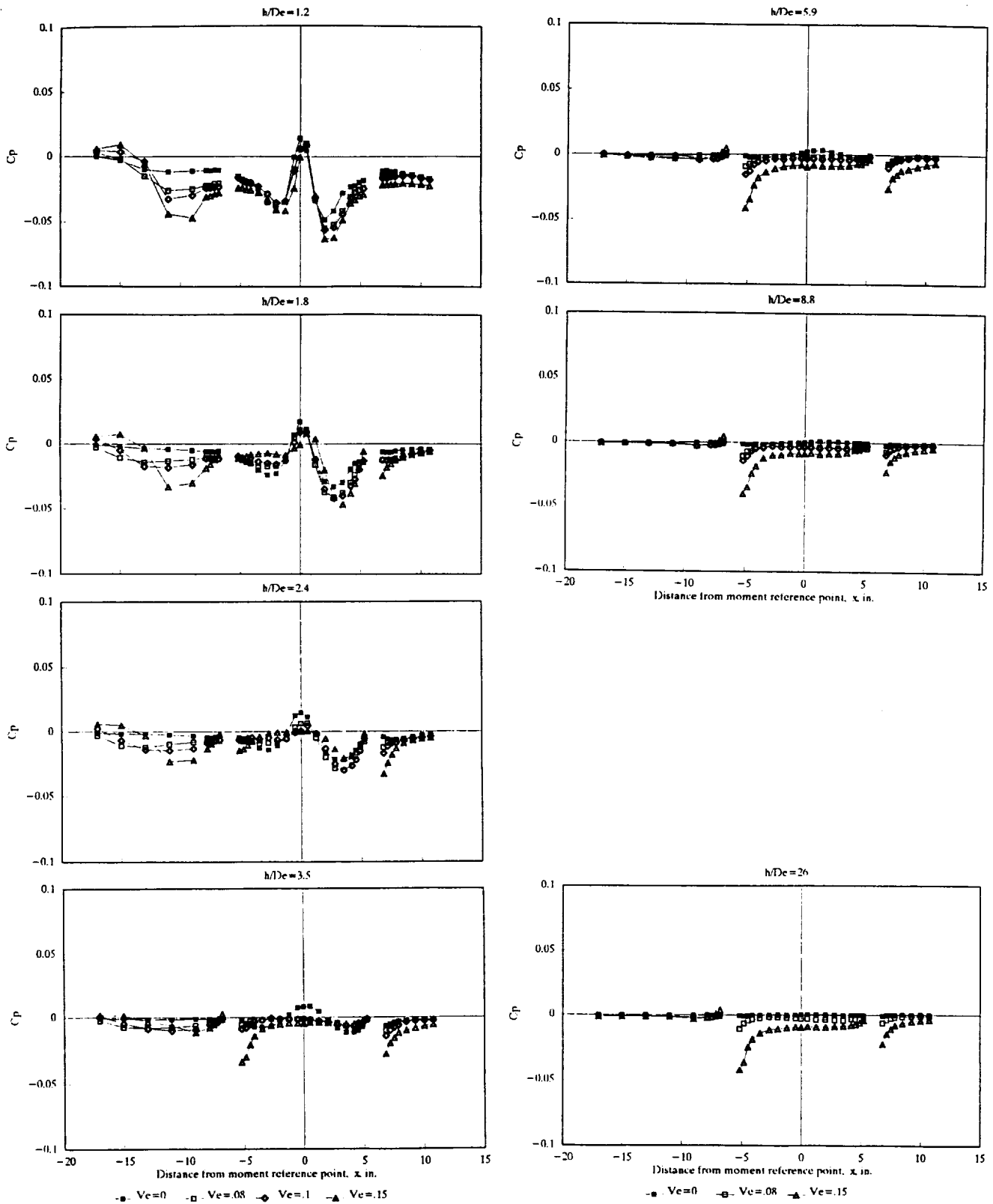
Figure 2.- Configuration of model of reference 14, showing locations of pressure taps and jets.



a) Centerline pressures on model and on ground
 b) Free stream upwash induced by ground vortex
 c) Effect of 'trapping' the ground vortex at low heights

Figure 3.- Schematic sketches of ground vortex induced flow fields and pressures induced.

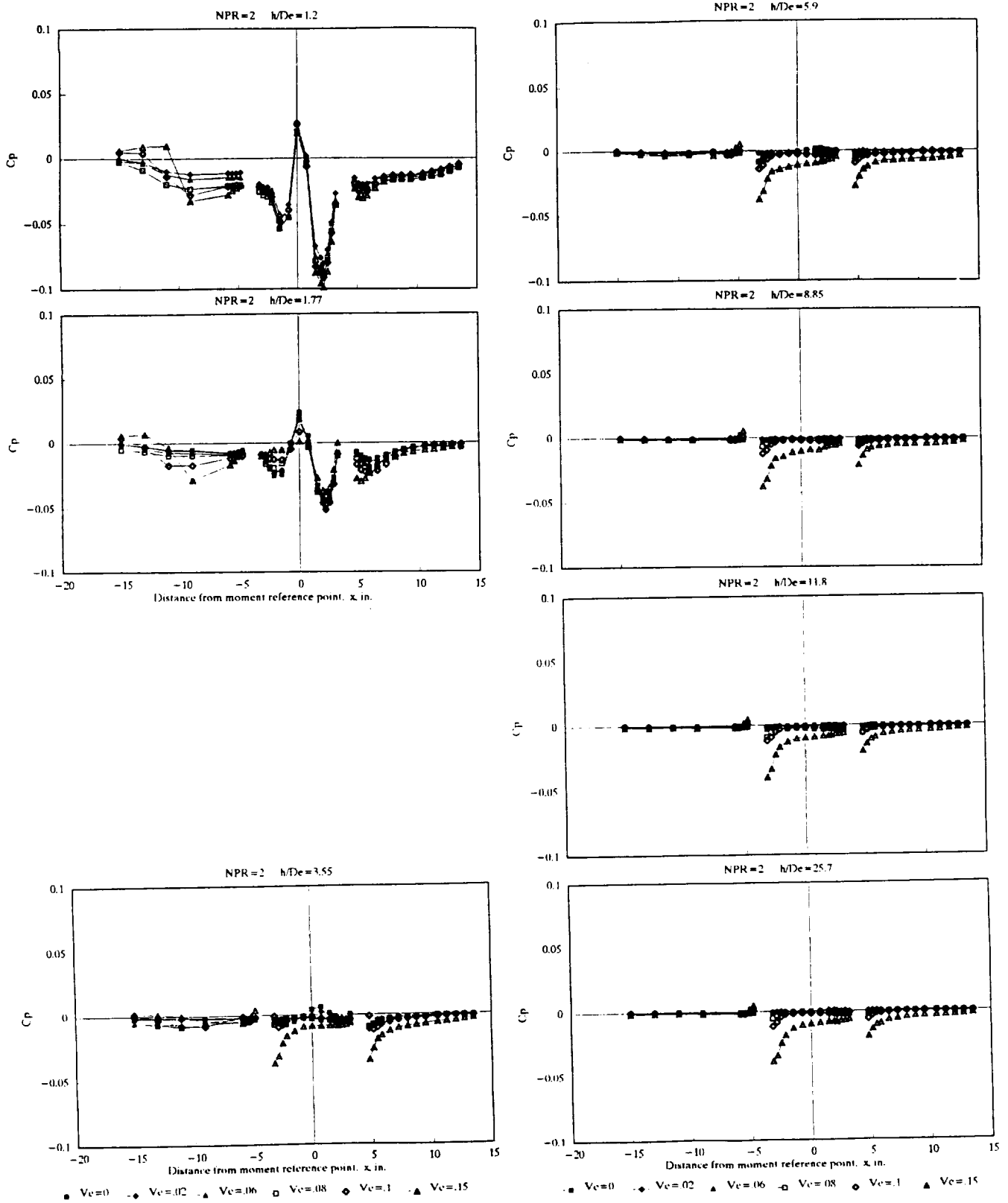
Centerline Press. Dist. — Conf. II



a) Configuration II - e/d = 5

Figure 4.- Effect of height and velocity ratio on the centerline pressure distribution.

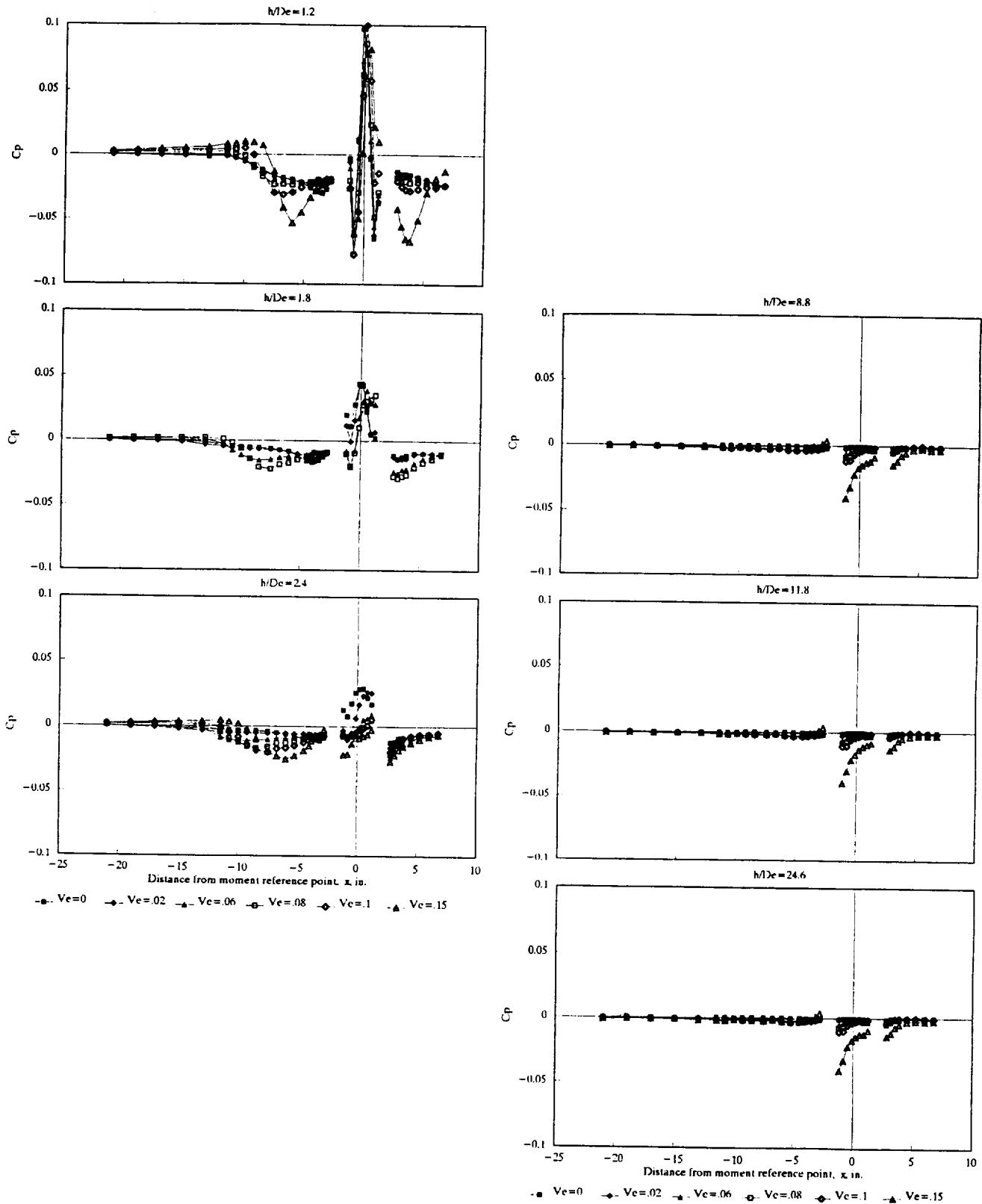
Centerline Press. Dist. — Conf. I



b) Configuration I - $e/d = 3.33$

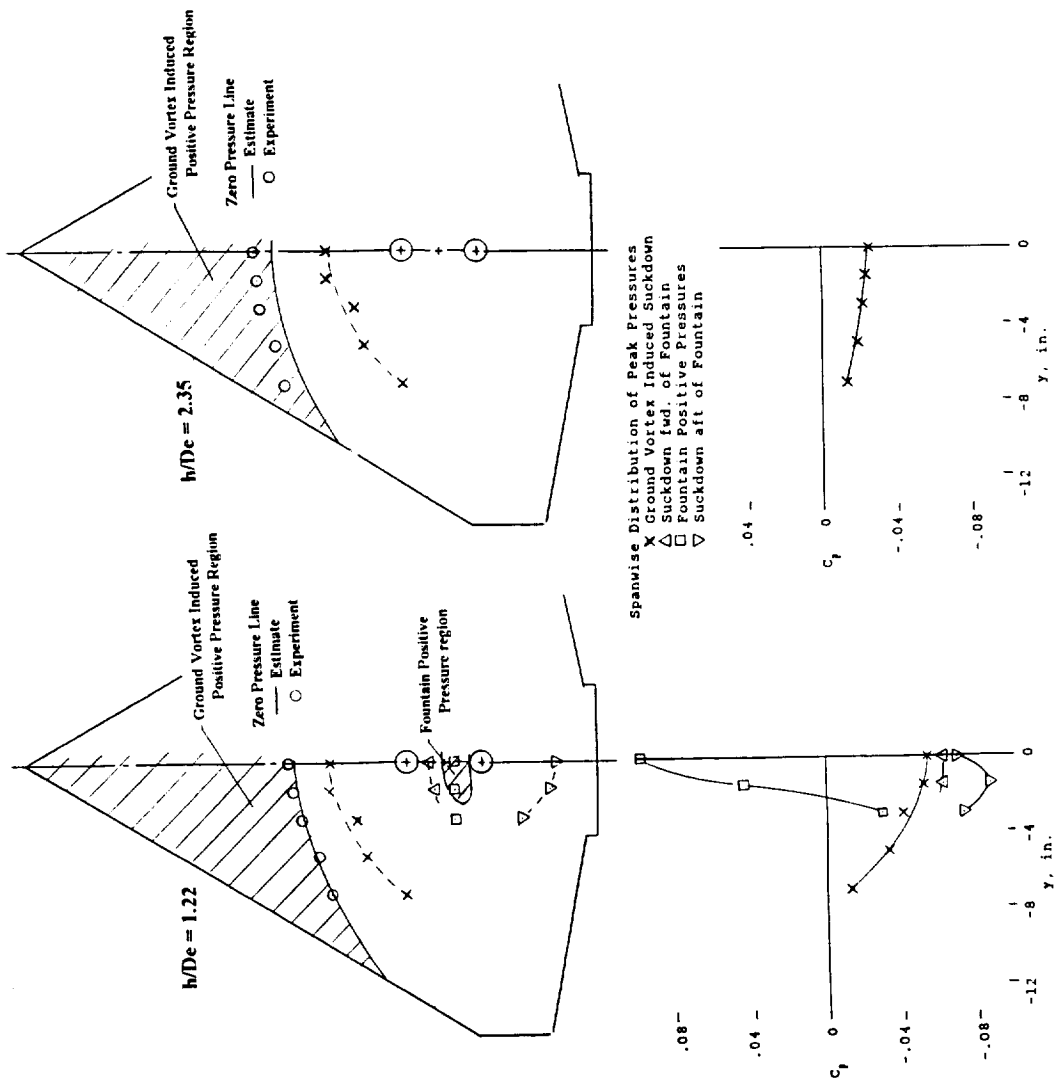
Figure 4.- Continued.

Centerline Press. Dist. — Conf. V



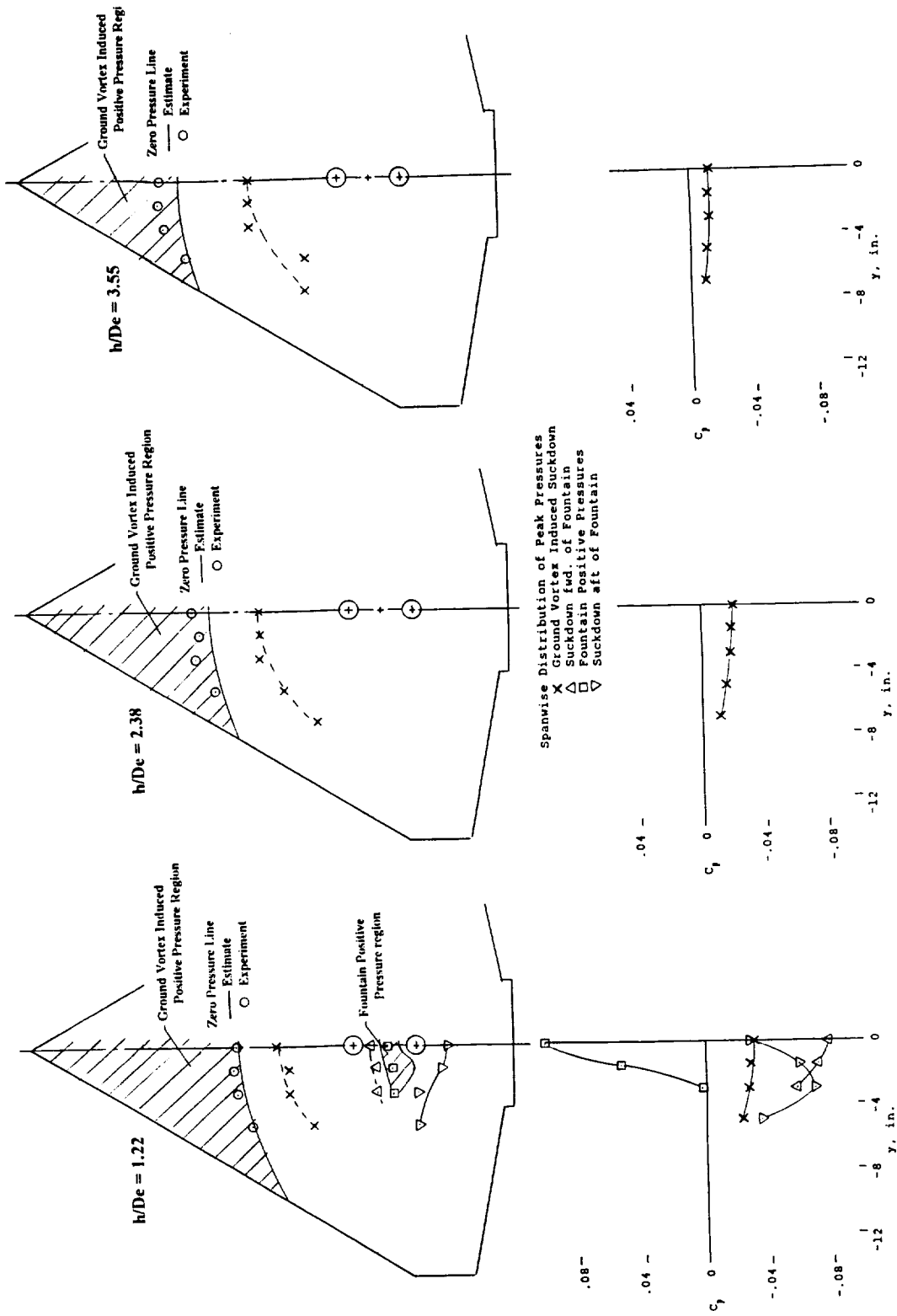
c) Configuration V - $e/d = 1.67$

Figure 4.- Concluded.



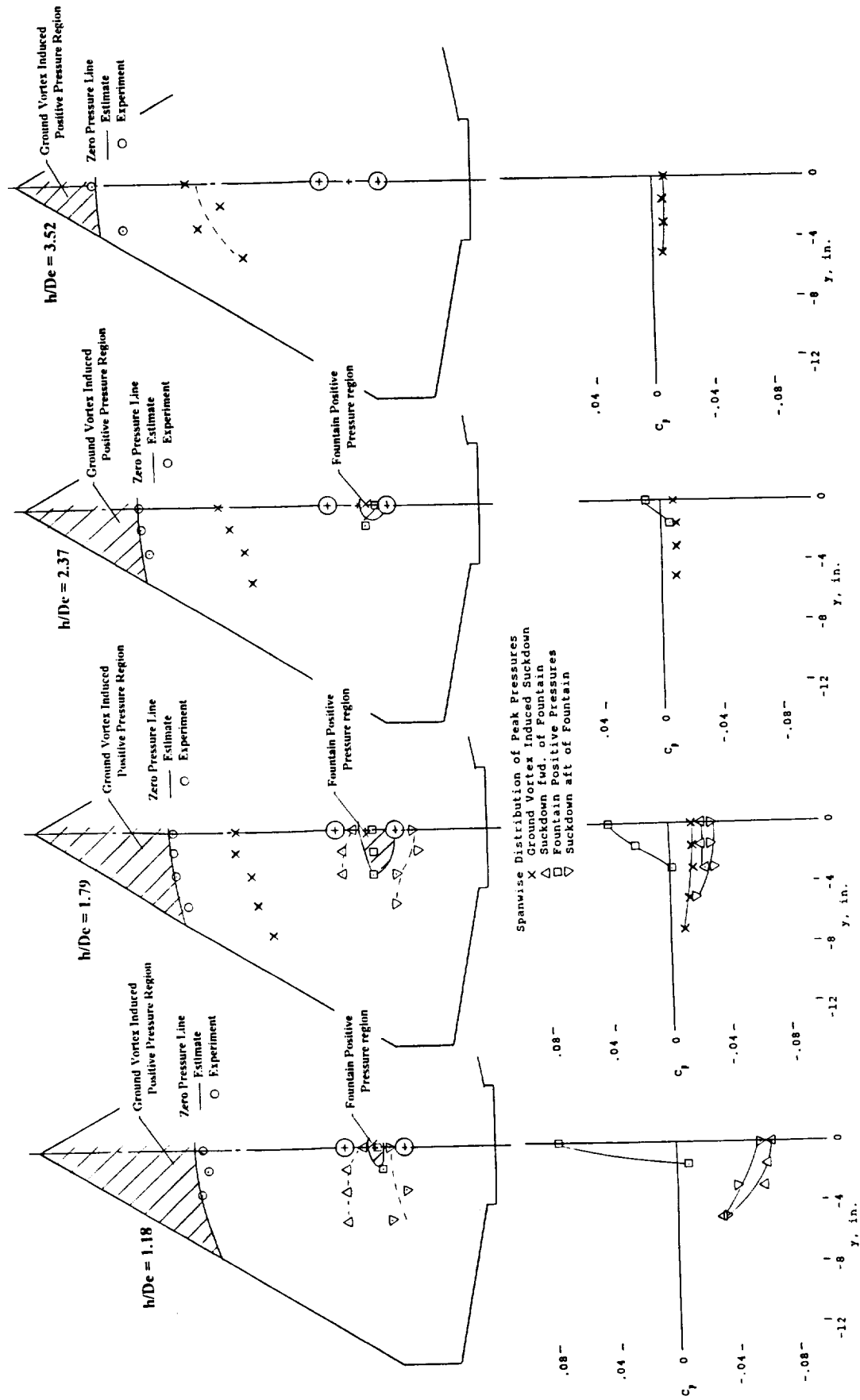
a) $V_e = .15$

Figure 5.- The effect of height and velocity ratio on the location and spanwise distribution of the ground vortex and fountain induced pressures on configuration V ($e/d = 1.67$).



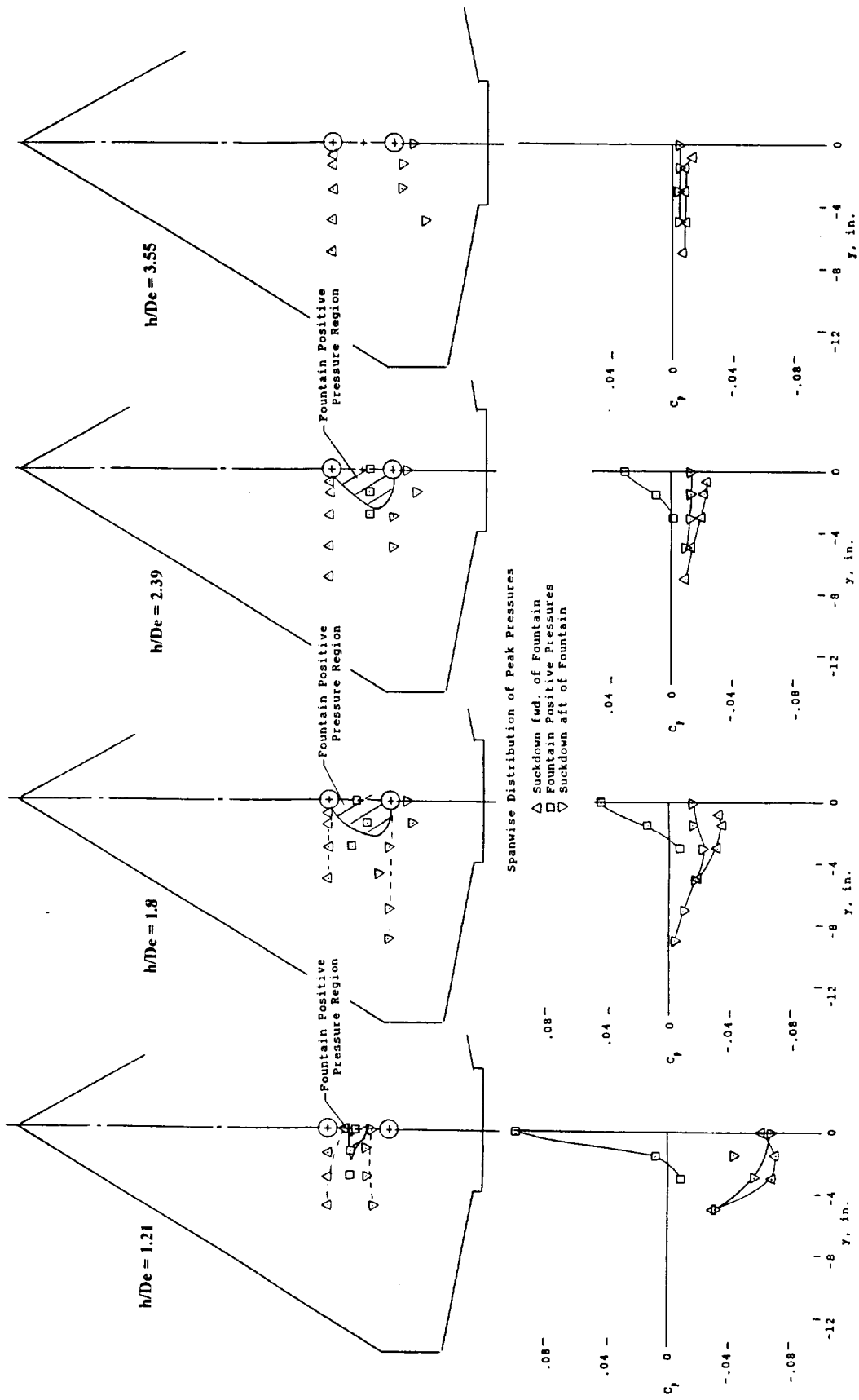
b) $V_e = .1$

Figure 5.- Continued.



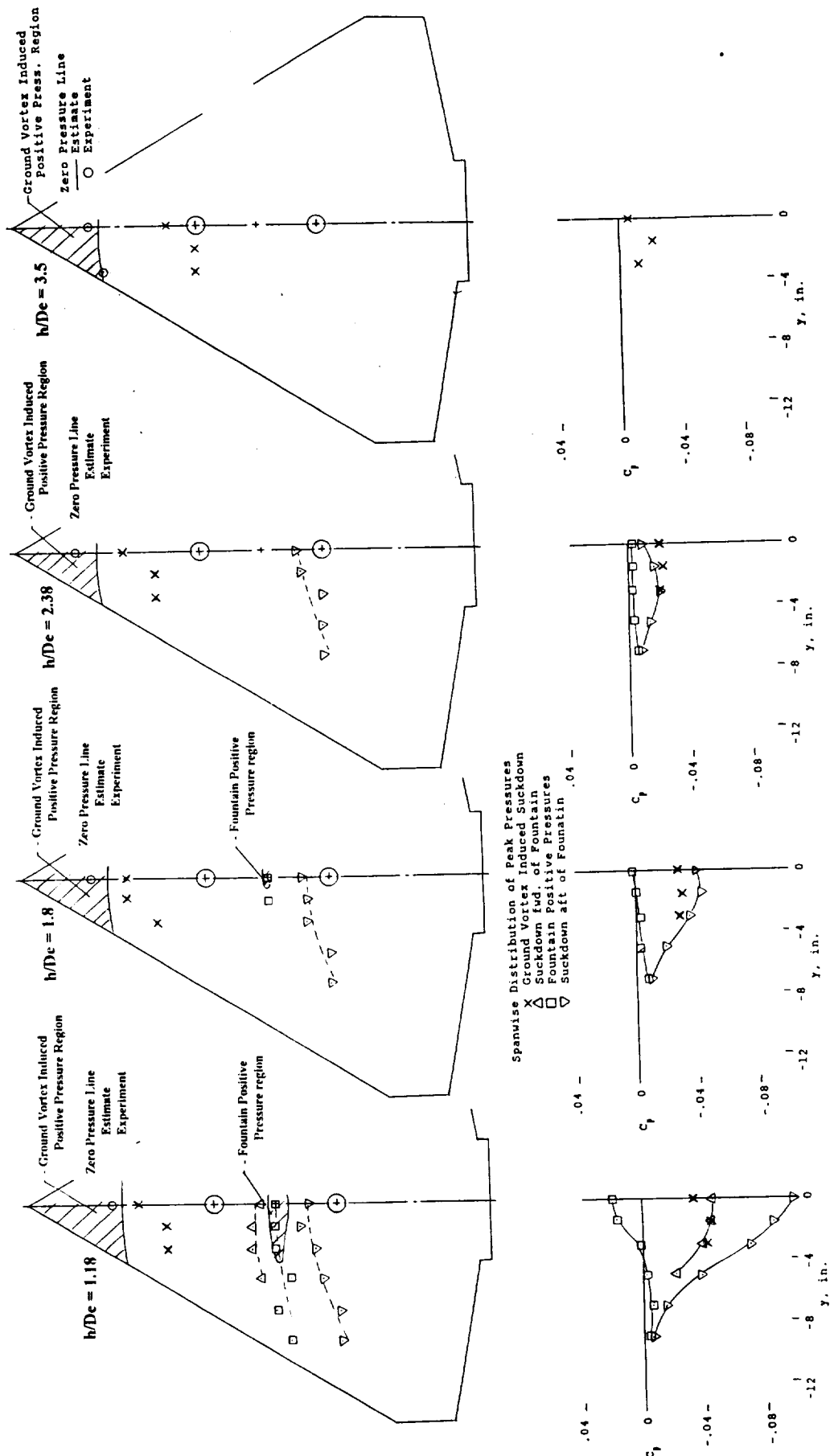
c) $V_e = .06$

Figure 5.- Continued.



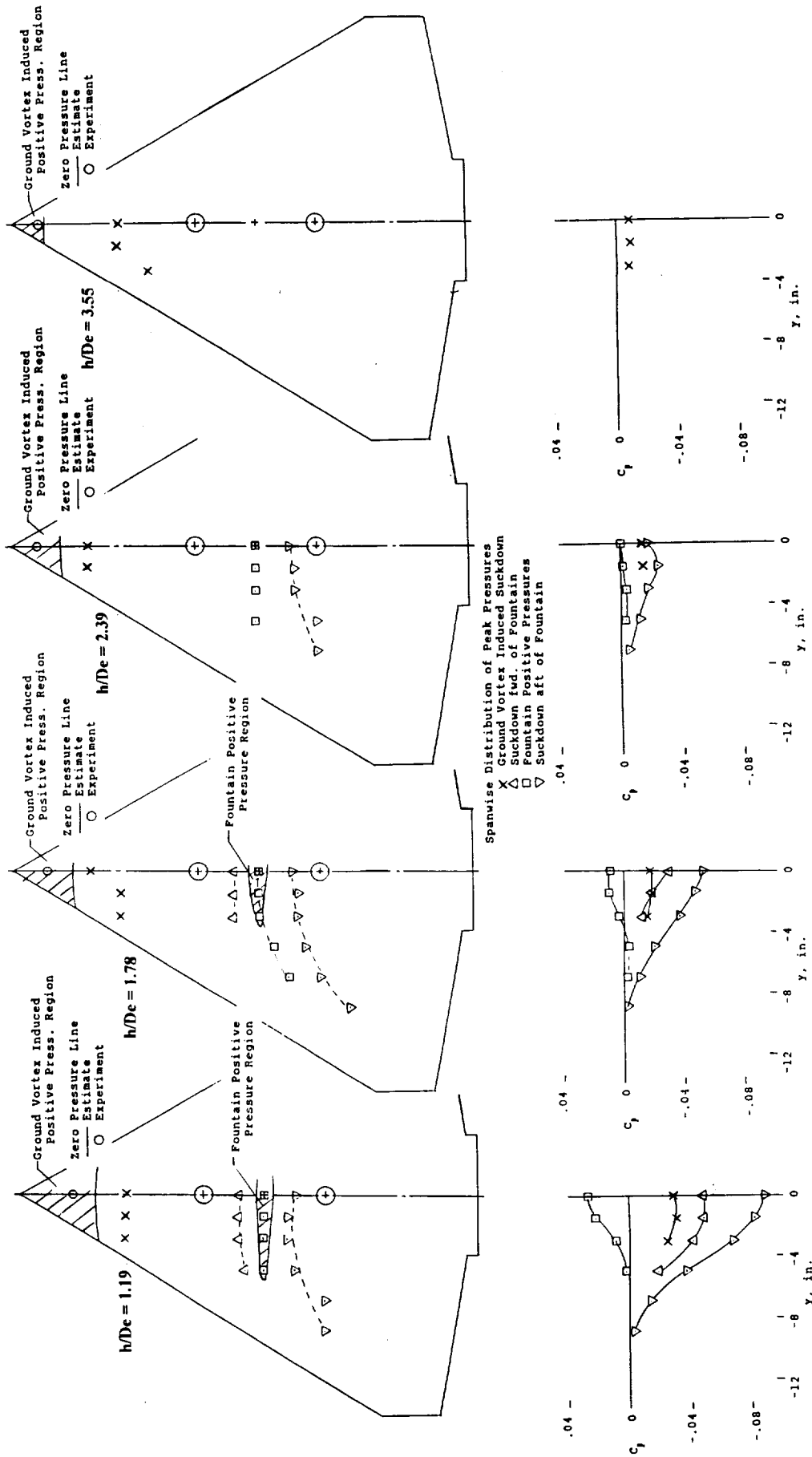
d) $V_e = 0$

Figured 5.- Concluded.



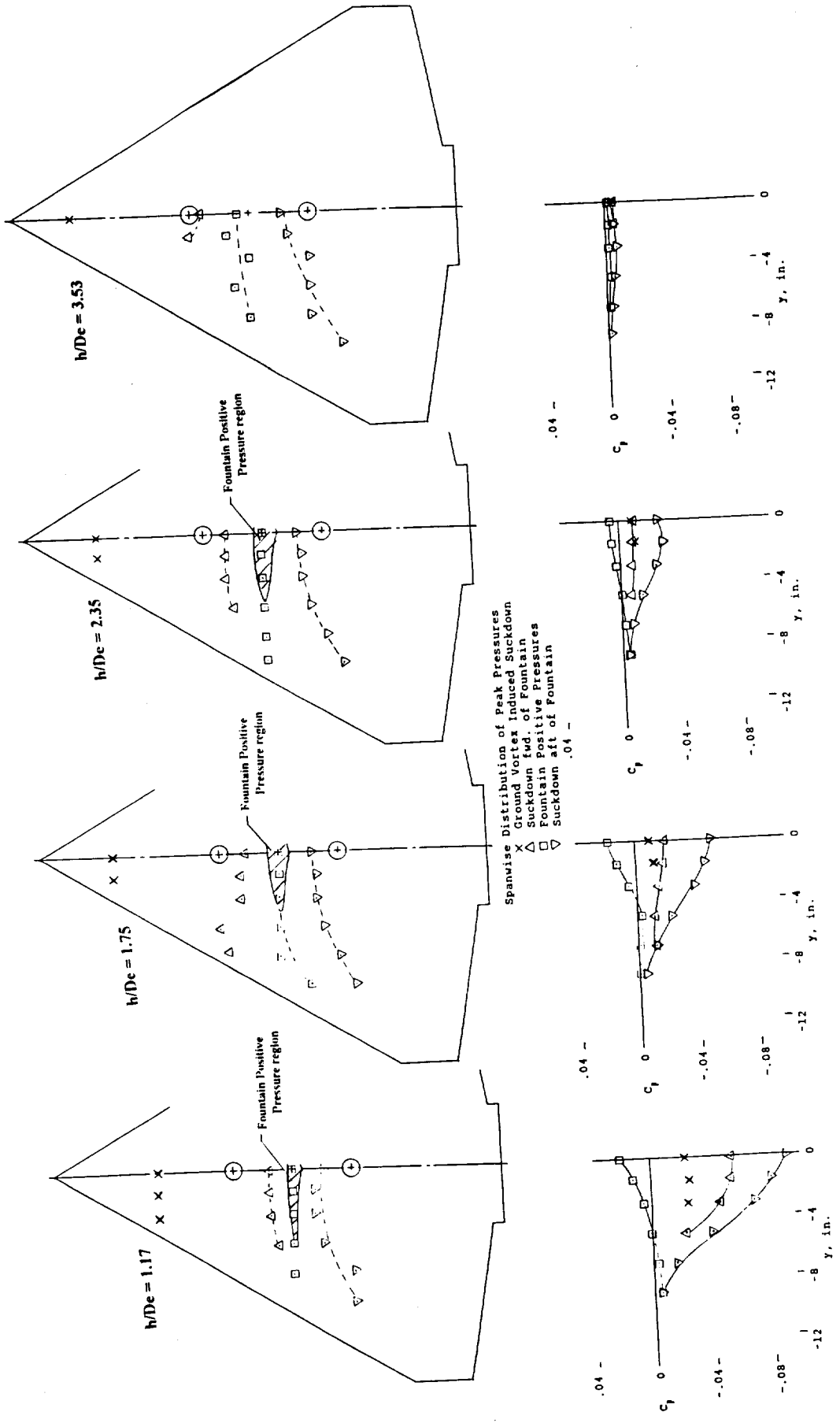
a) $V_e = .15$

Figure 6.- The effect of height and velocity ratio on the location and spanwise distribution of the ground vortex and fountain induced pressures on configuration I ($e/d = 3.33$).



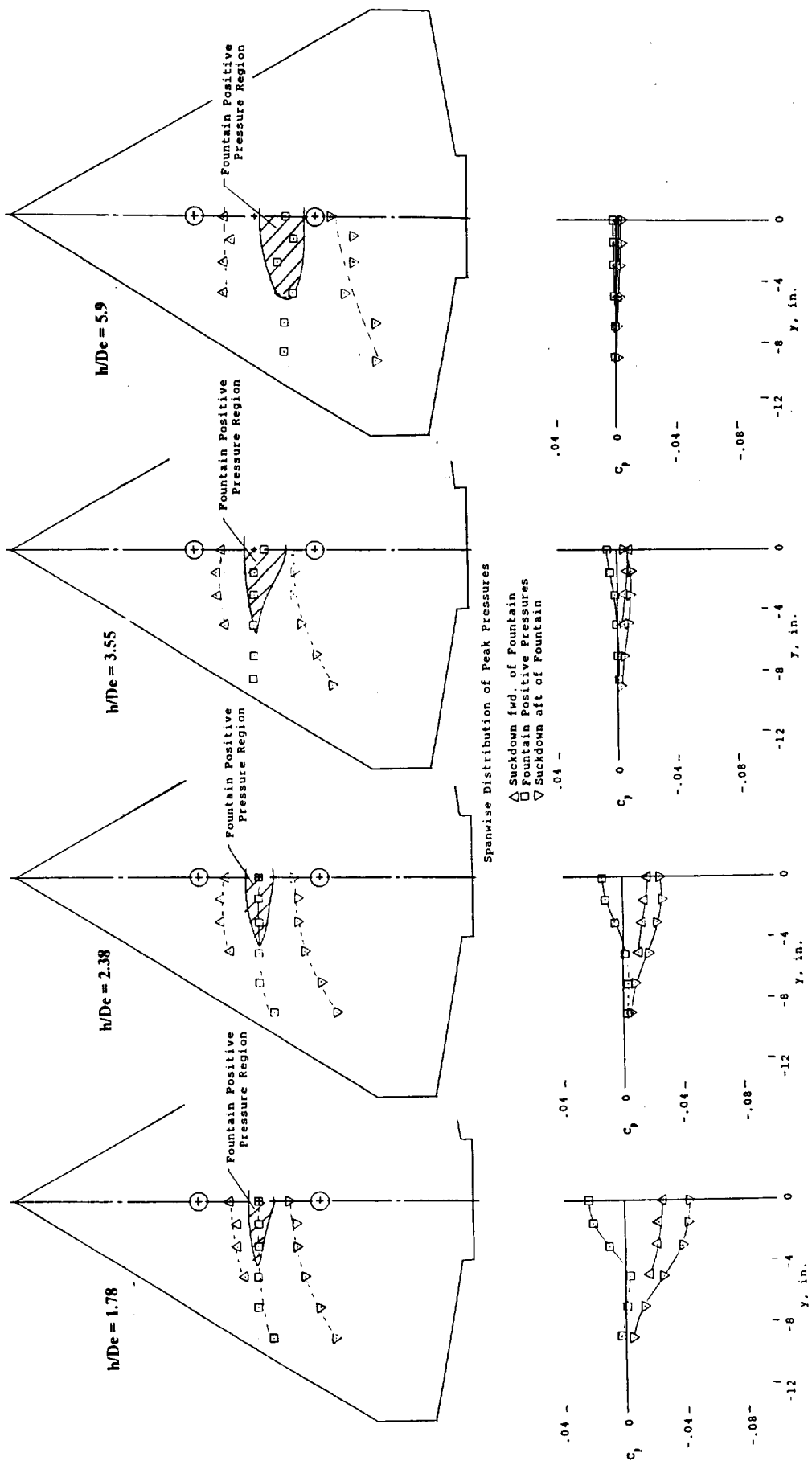
b) $V_e = .1$

Figure 6.- Continued.

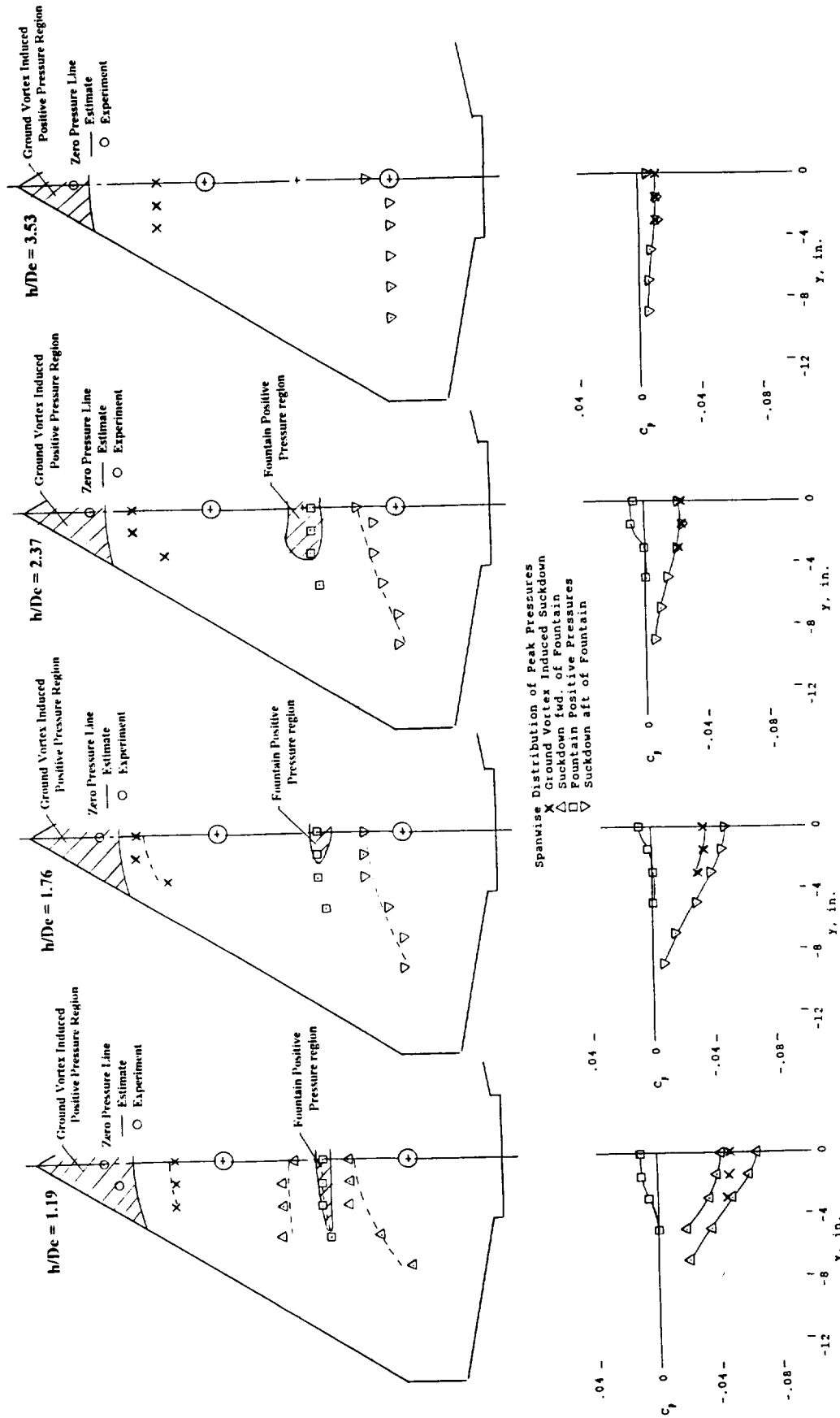


c) $V_e = .06$

Figure 6.- Continued.

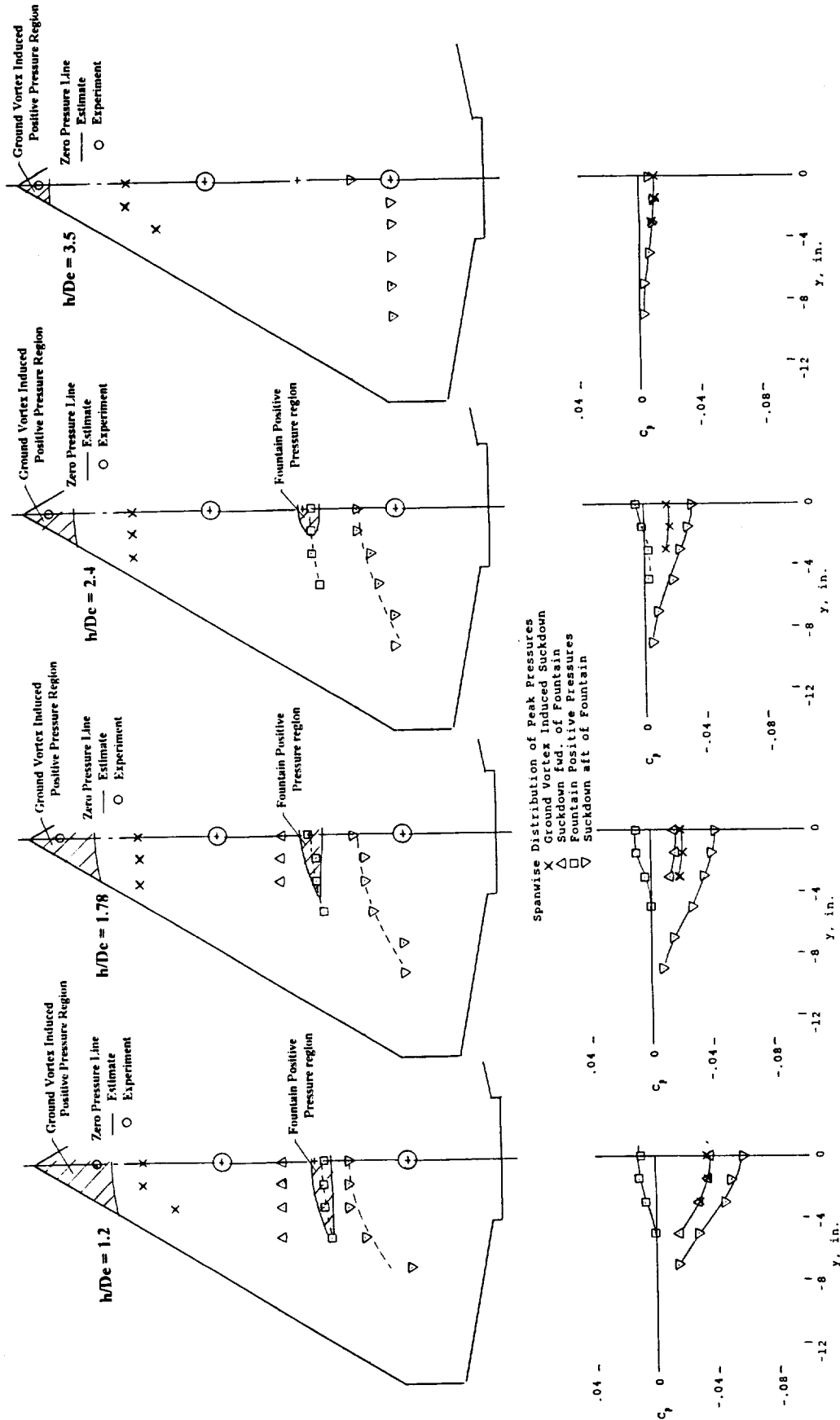


d) $V_e = 0$
 Figured 6.- Concluded.



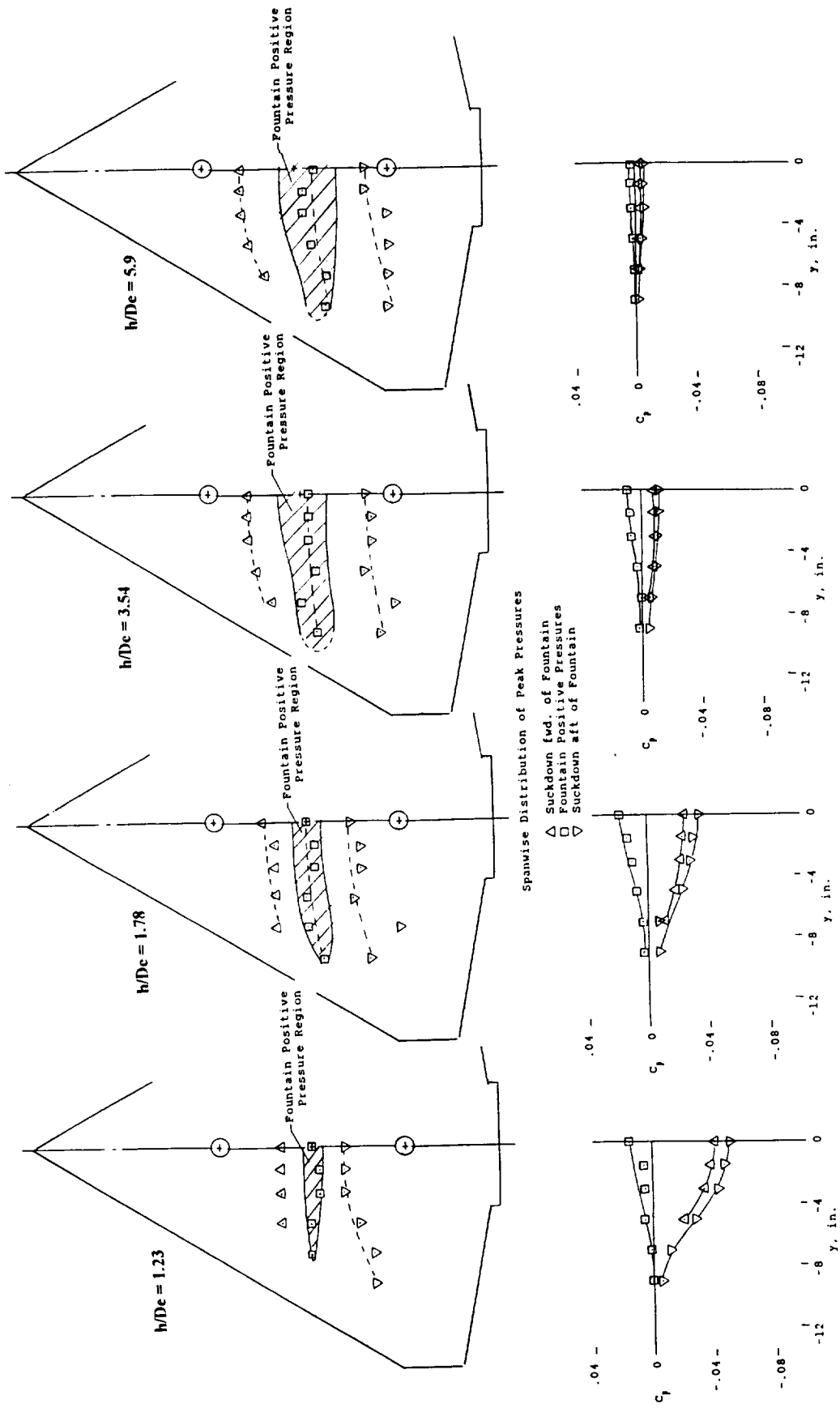
a) $V_e = .15$

Figure 7.- The effect of height and velocity ratio on the location and spanwise distribution of the ground vortex and fountain induced pressures on configuration II ($e/d = 3.33$).



b) $V_e = .1$

Figure 7.- Continued.



c) $V_e = 0$

Figured 7.- Concluded.

$$\left(\frac{\Delta L}{T}\right)_{est} = \left(\frac{\Delta L}{T}\right)_{h,s} + \left(\frac{\Delta L}{T}\right)_w + \left(\frac{\Delta L}{T}\right)_f + \left(\frac{\Delta L}{T}\right)_{GV,p} + \left(\frac{\Delta L}{T}\right)_{GV,n} + \left(\frac{\Delta L}{T}\right)_{us} + \left(\frac{\Delta L}{T}\right)_{w,t} + \left(\frac{\Delta L}{T}\right)_{cf}$$

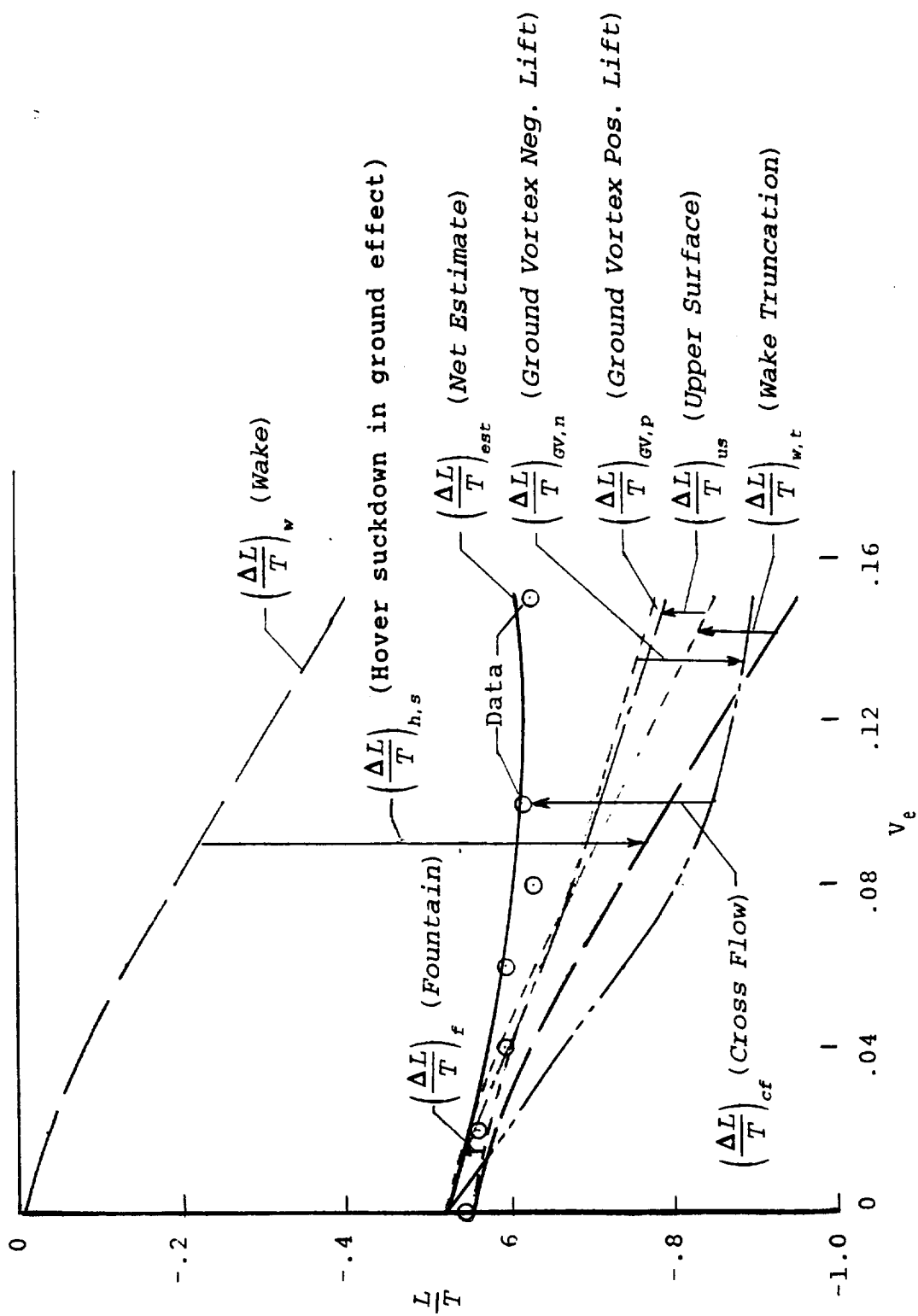


Figure 8.- Schematic of the elements used in the analysis.

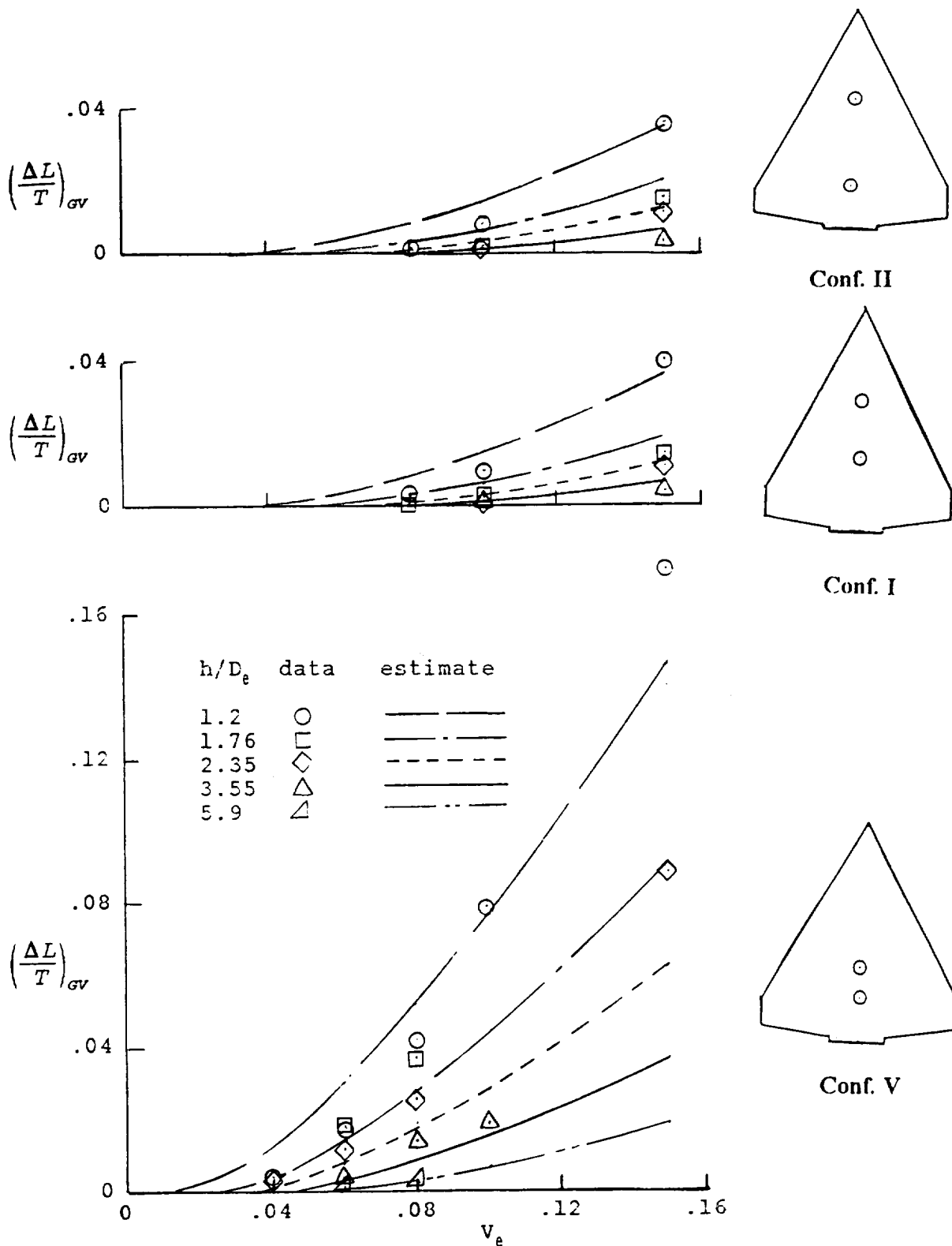


Figure 9.- Comparison of estimated positive lift induced by the ground vortex with the experimental data from integration of pressures forward of the zero pressure line.

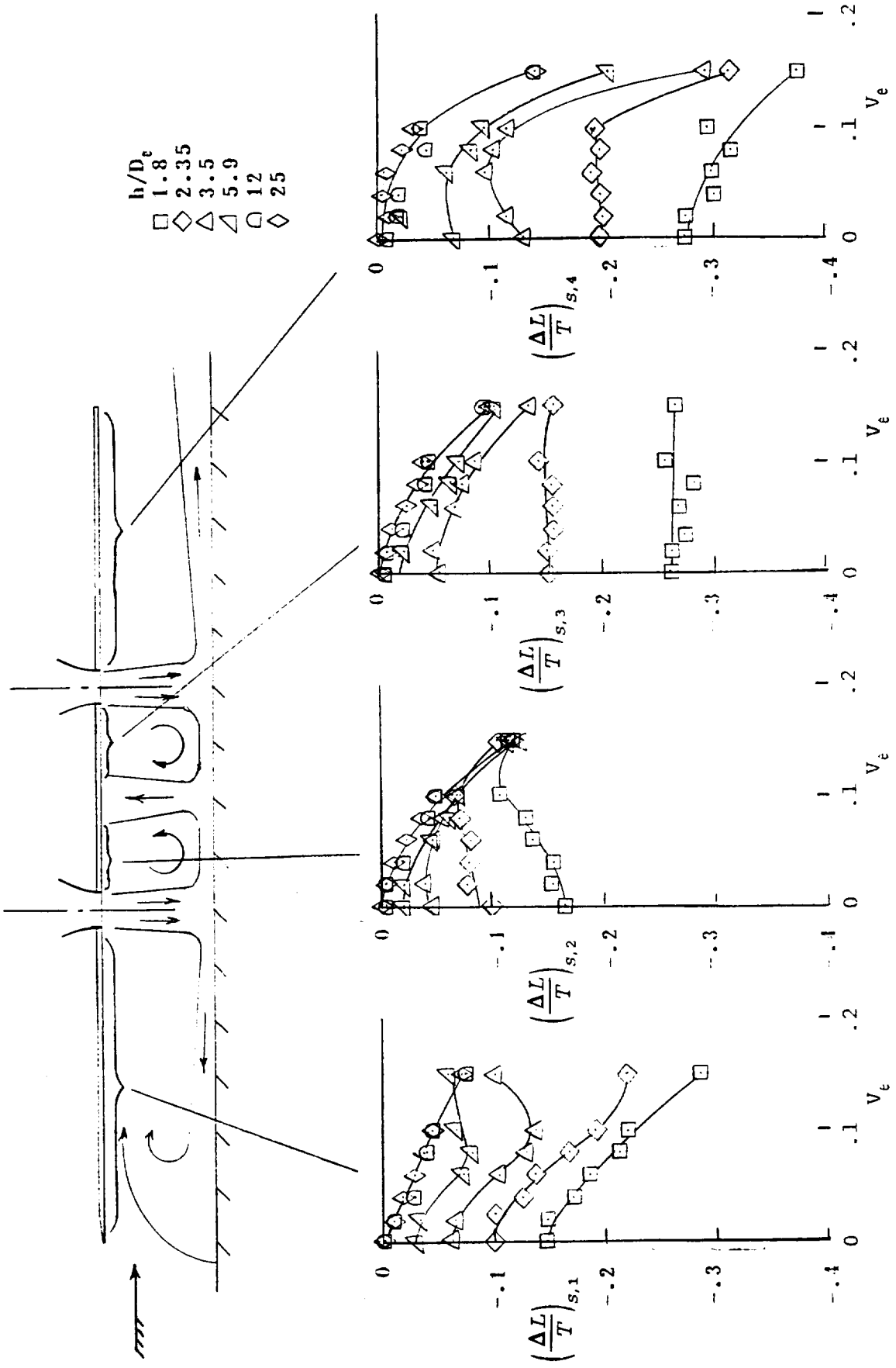


Figure 10.- Effect of height and crossflow velocity ratio on the lift loss induced on the lower surface.

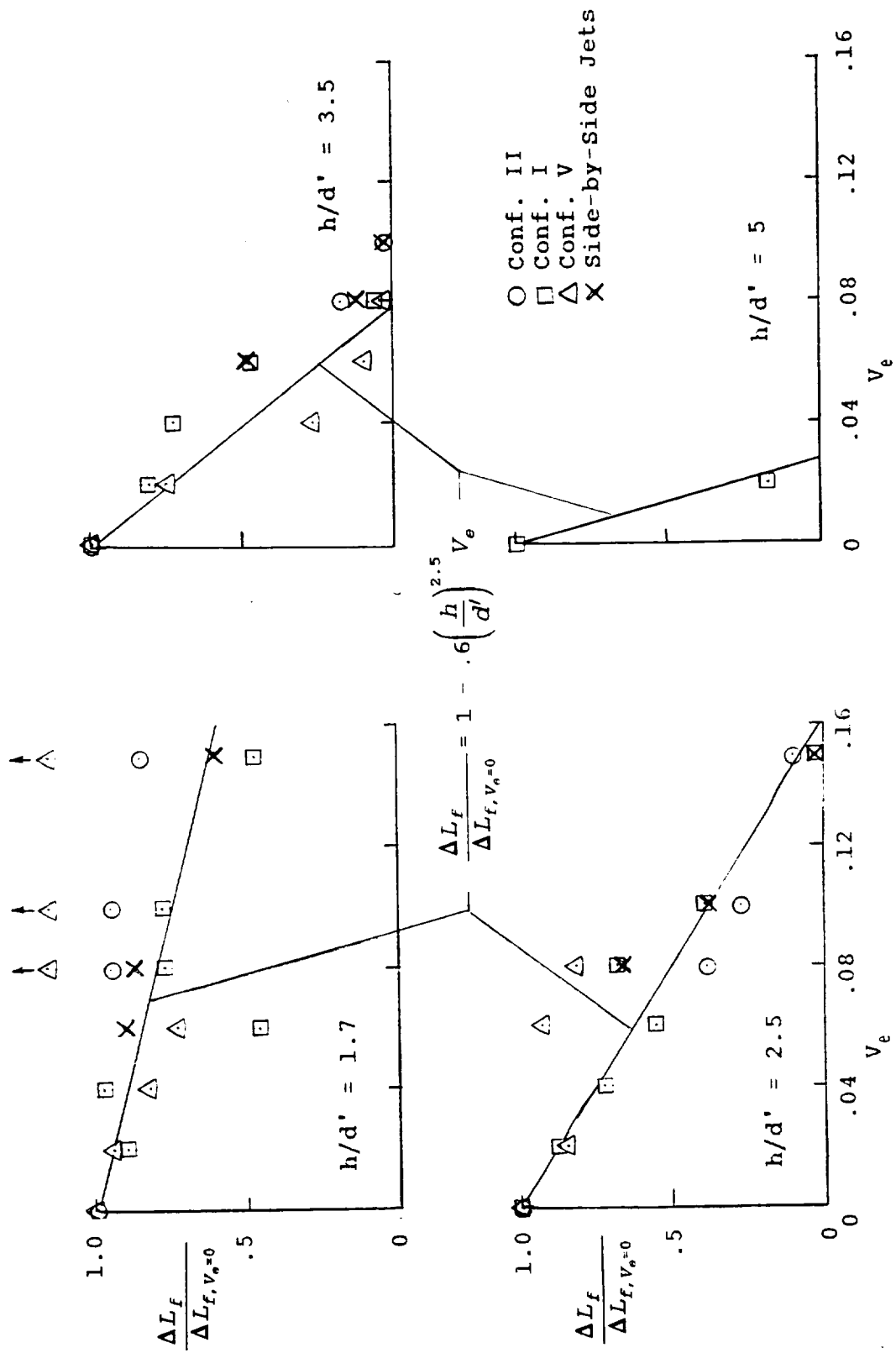
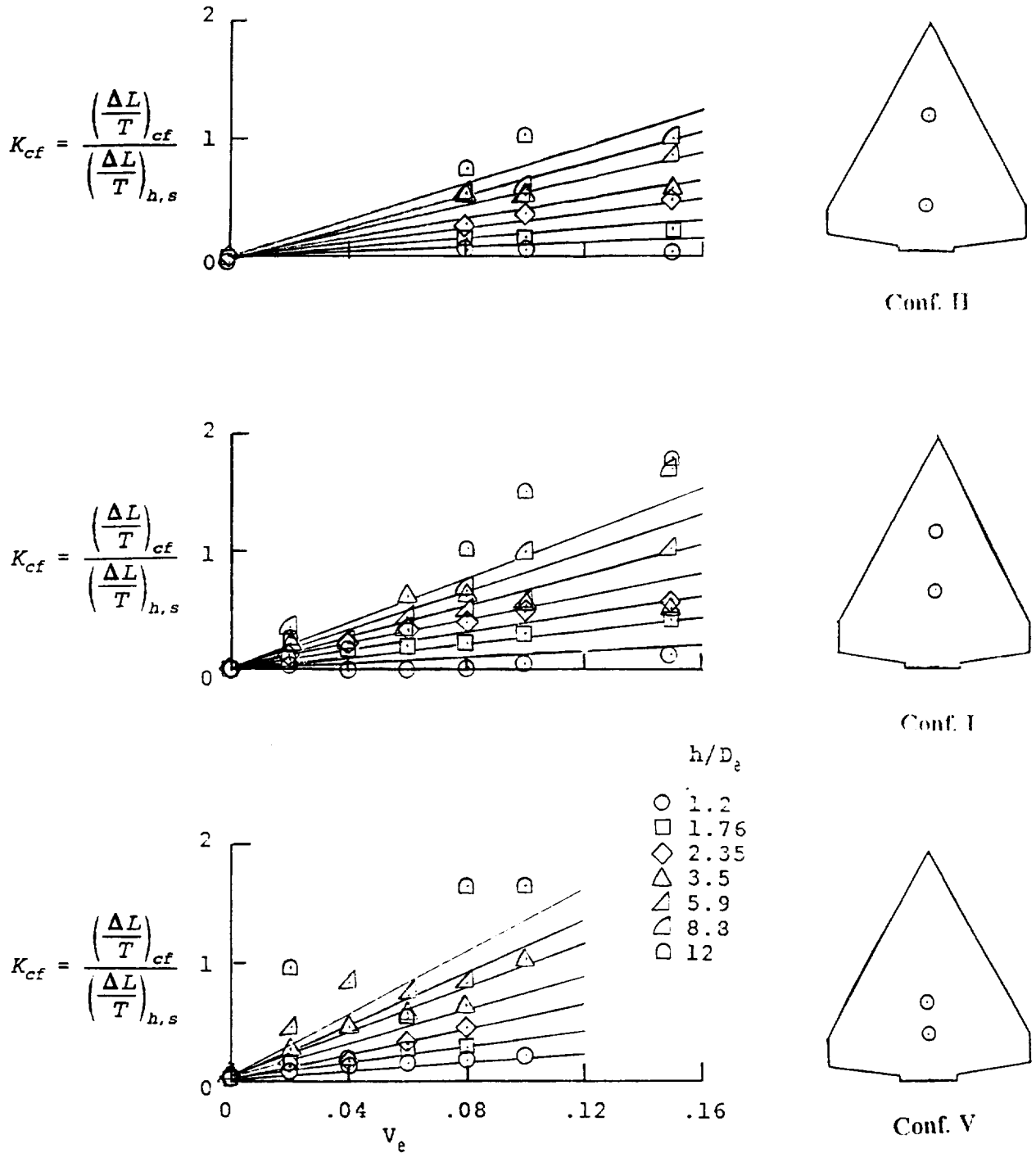
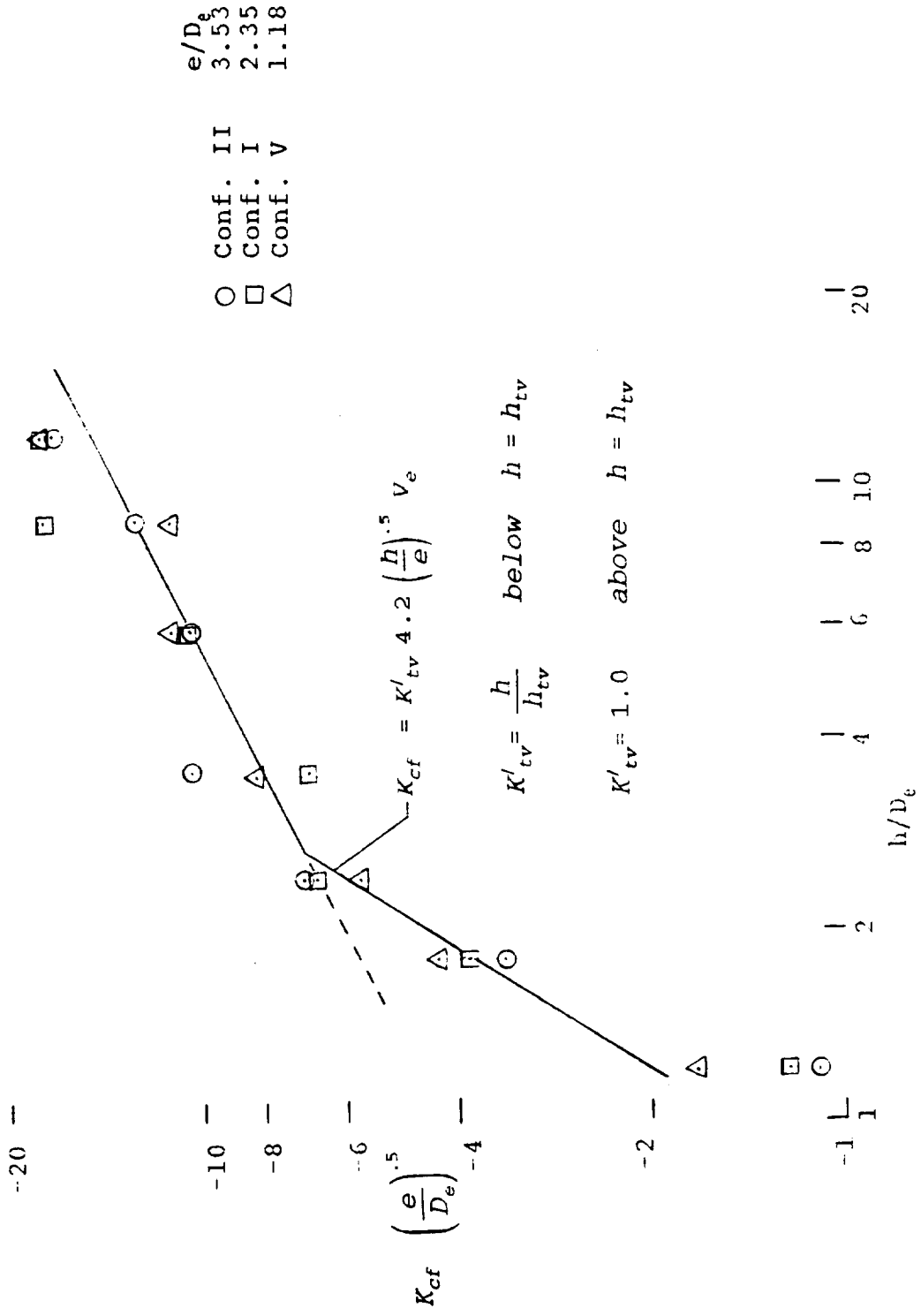


Figure 11.- Effect of crossflow in reducing the positive lift induced by impingement of the fountain flow.



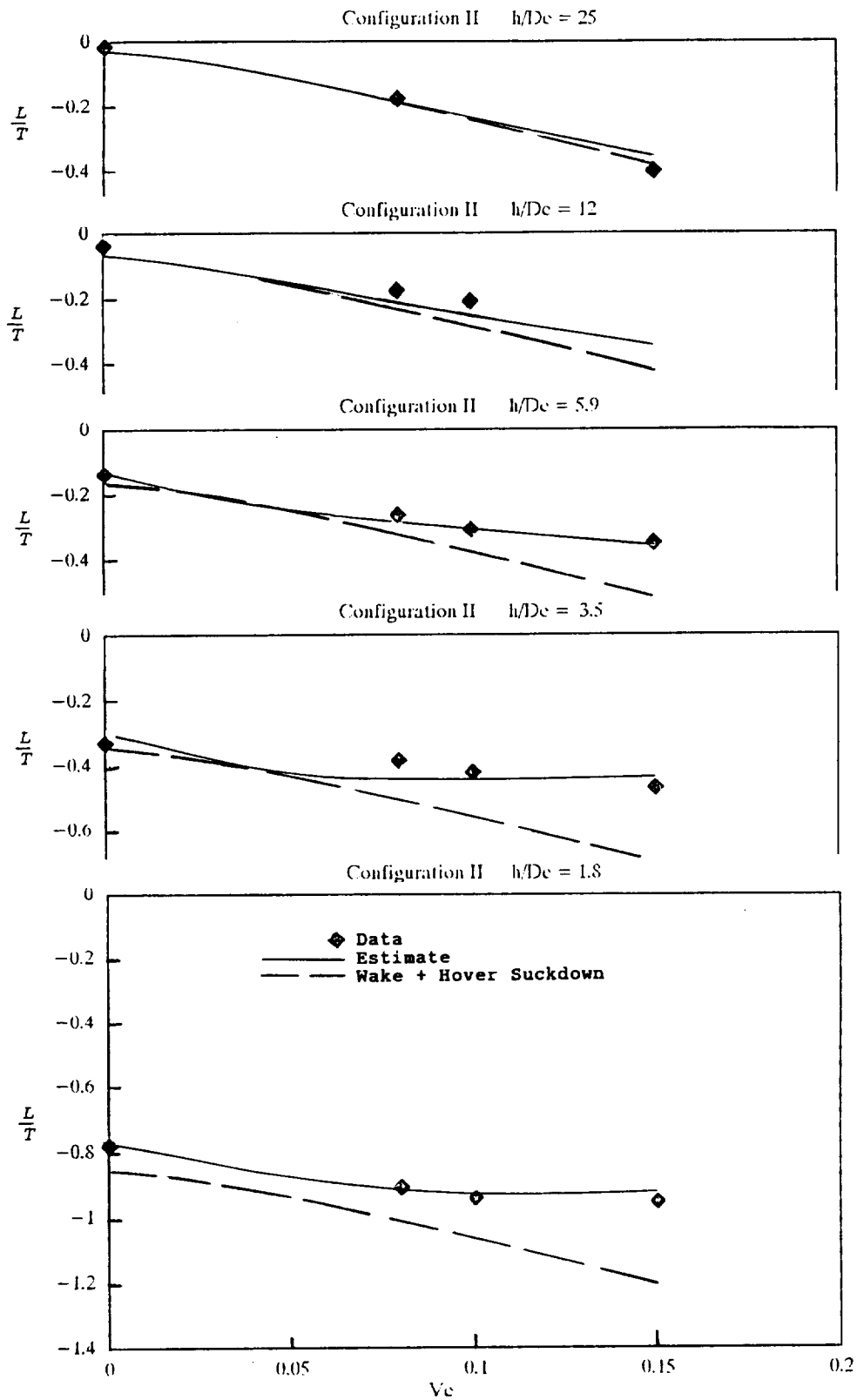
a) Effect of velocity ratio and configuration.

Figure 12.- Effect of height and crossflow velocity on the ratio of the crossflow increment of lift loss to the suckdown lift induced in hover.



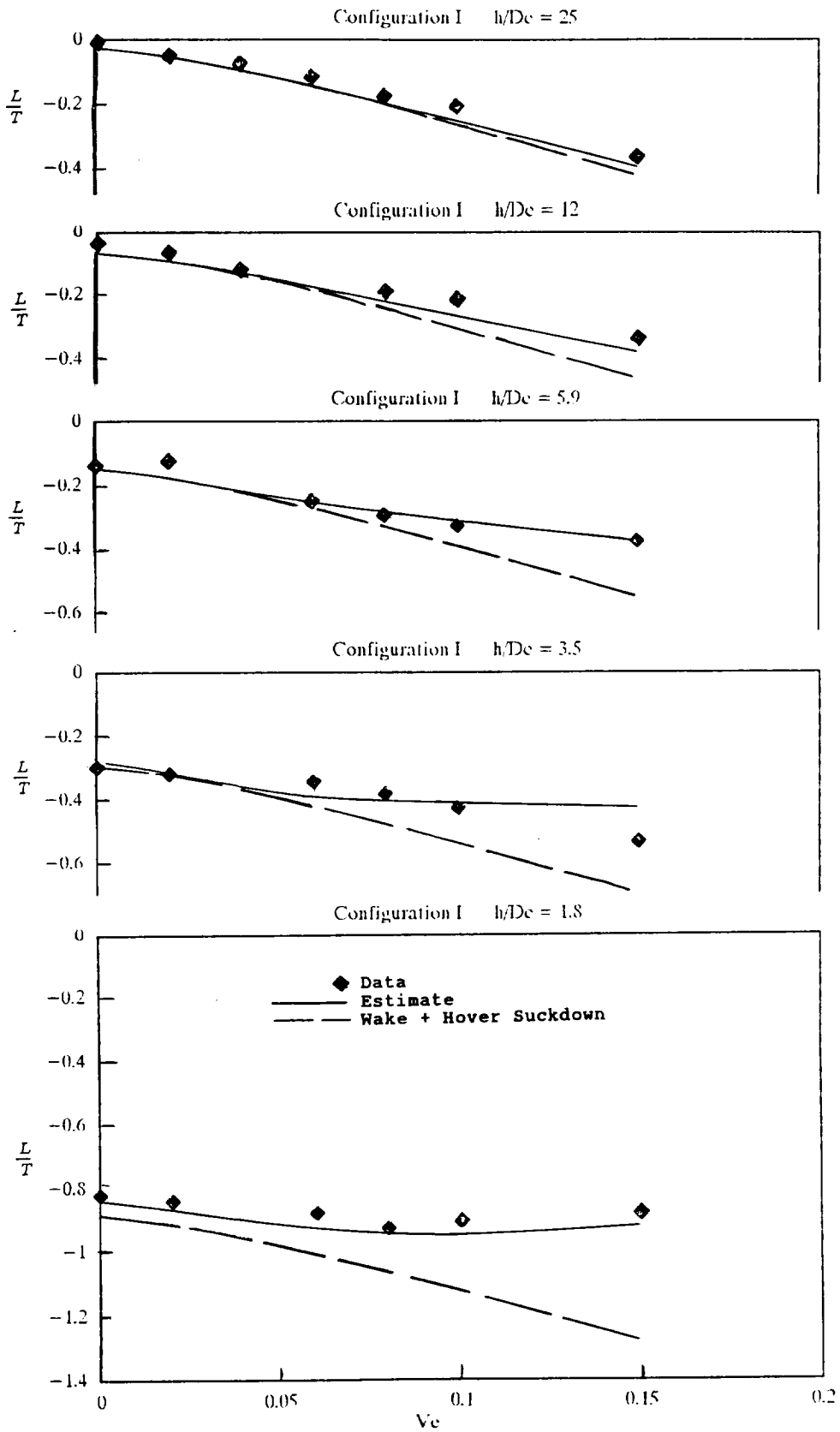
b) Effect of height.

Figure 12.- Concluded.



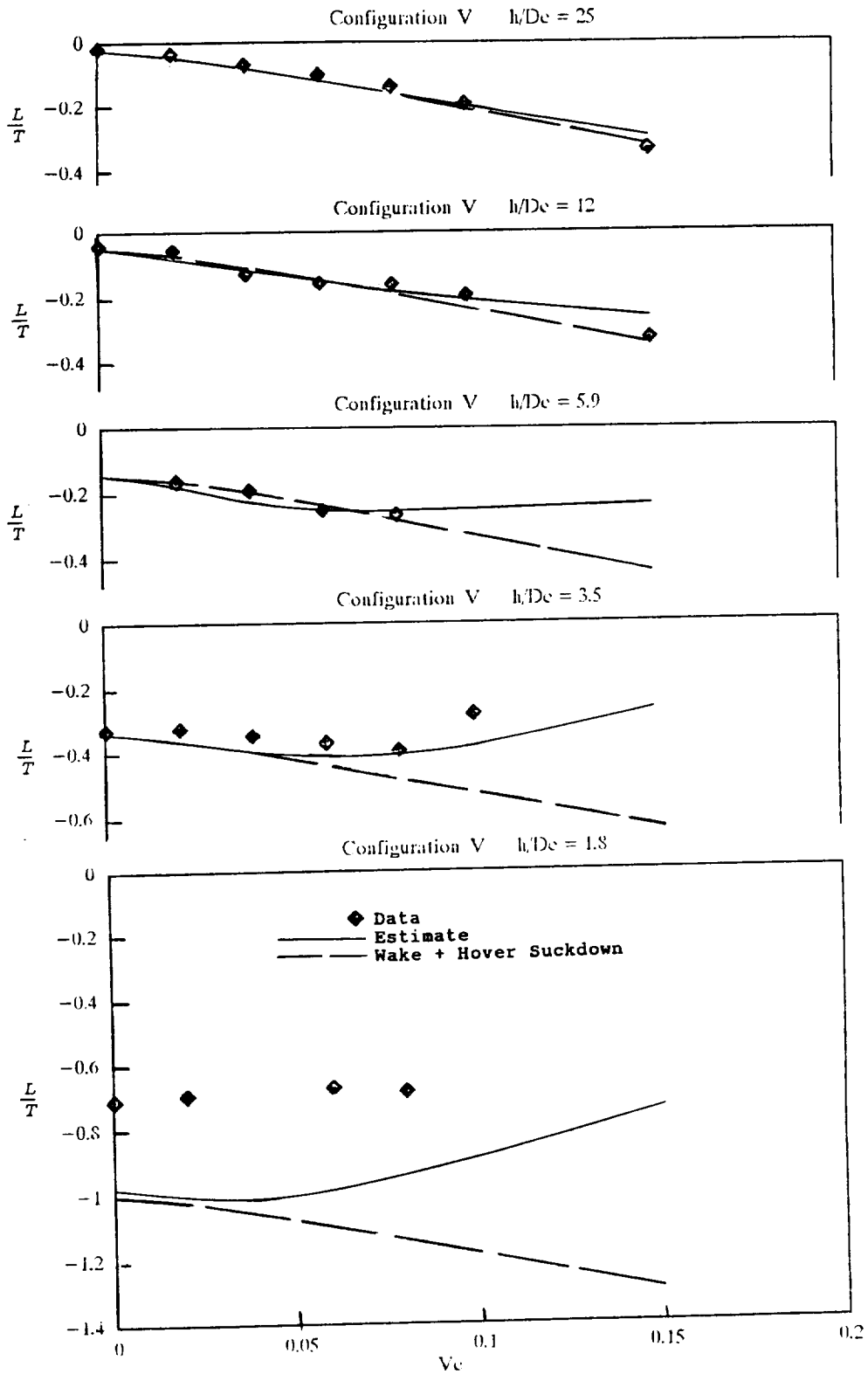
a) Configuration II - $e/d = 5$

Figure 13.- Comparison of estimated net lift loss with experimental data.



b) Configuration I - $e/d = 3.33$

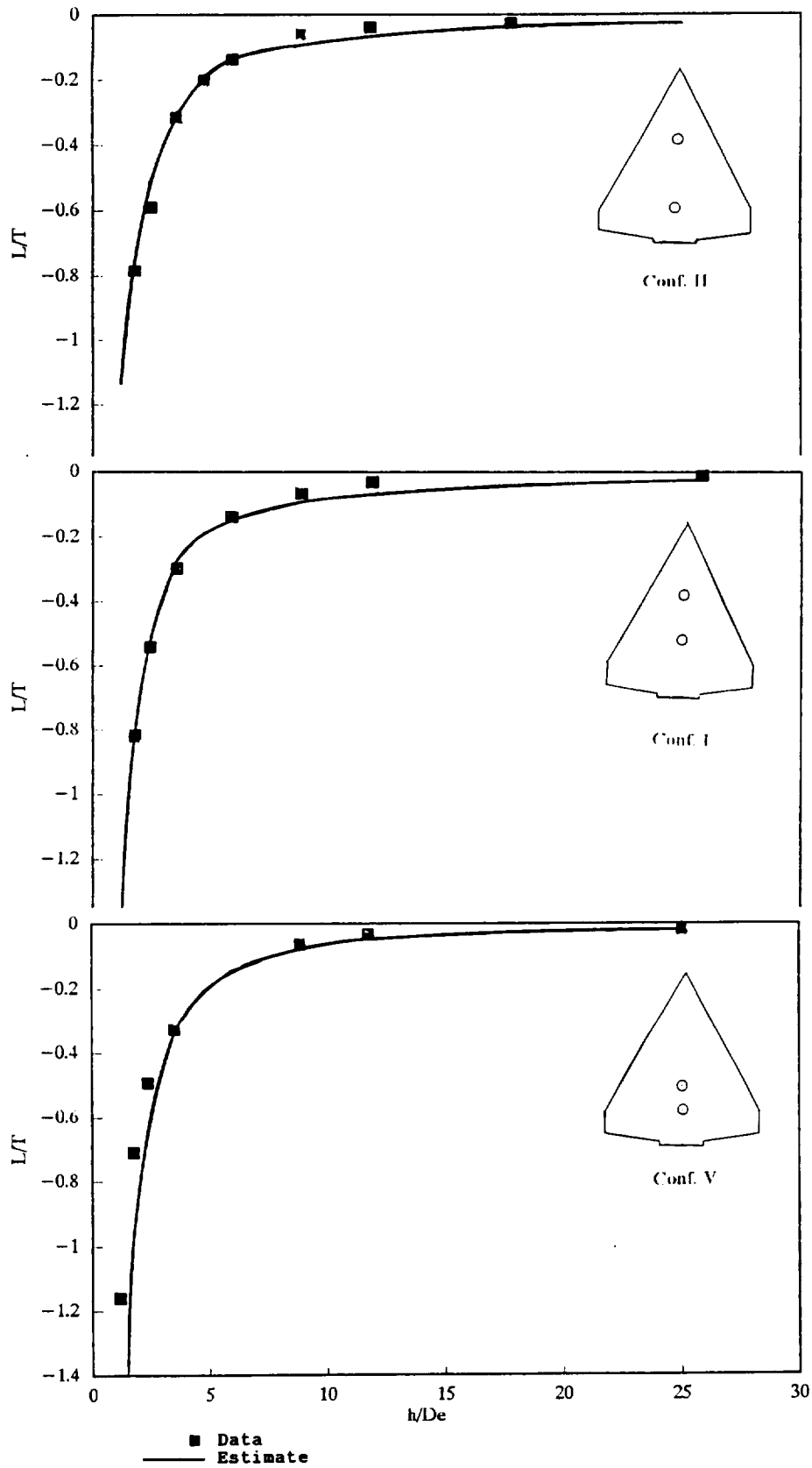
Figure 13.- Continued.



c) Configuration V - $e/d = 1.67$

Figure 13.- Concluded.

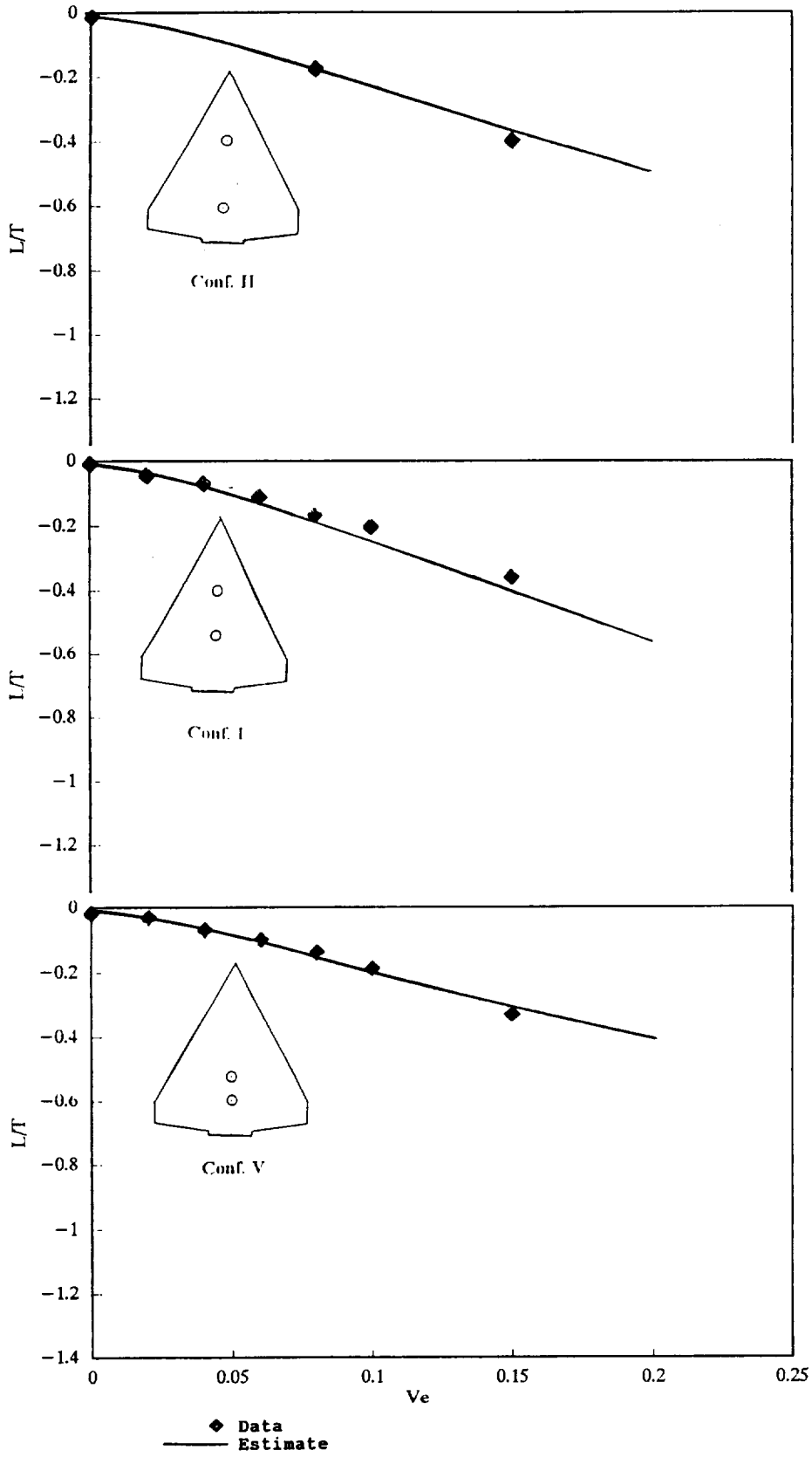
Hover Estimate



a) Hover - ref. 9 estimate.

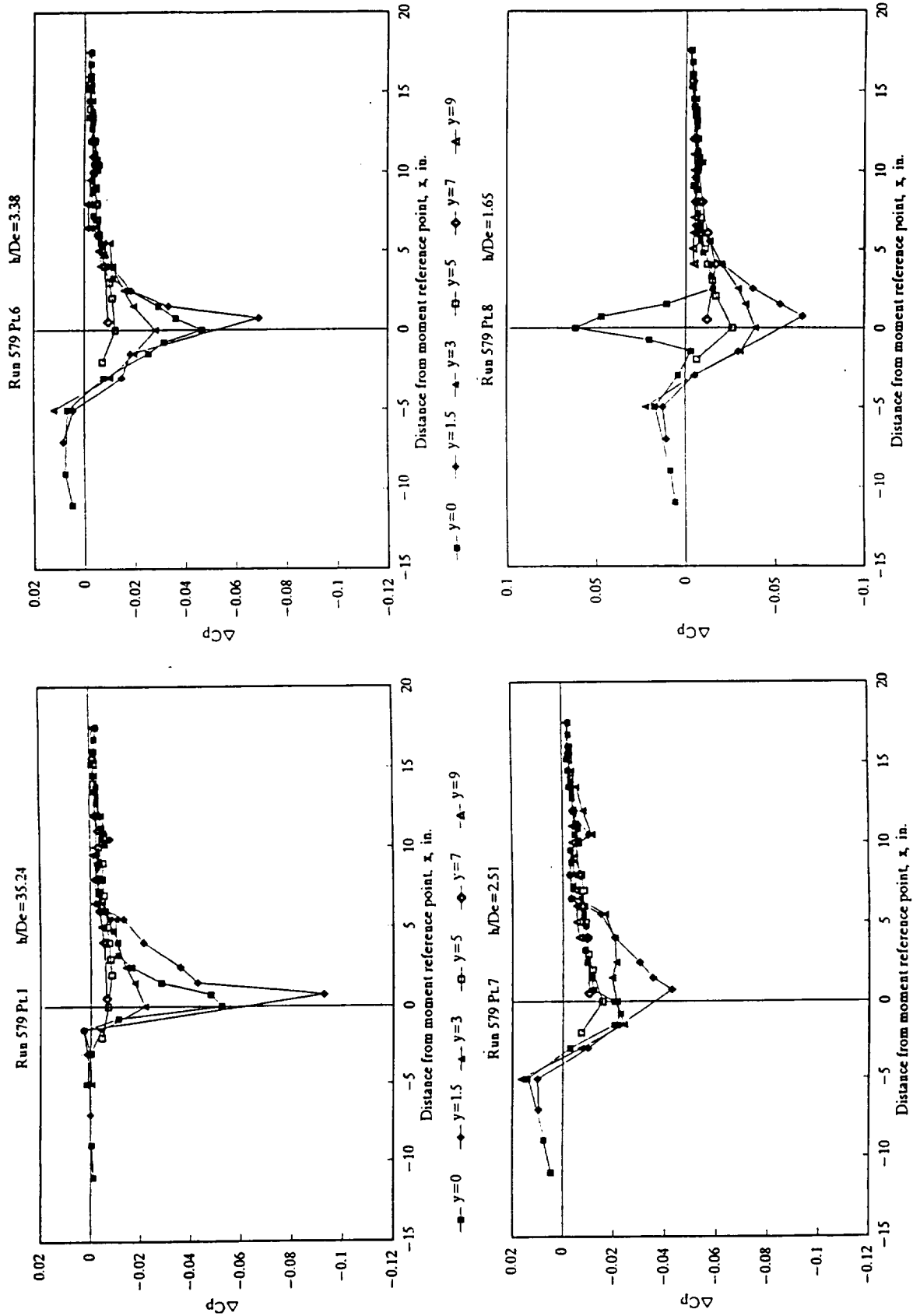
Figure 14.- Comparison of Hover and Out-of-Ground Effect estimates with data.

Transition – Out of Ground Effect



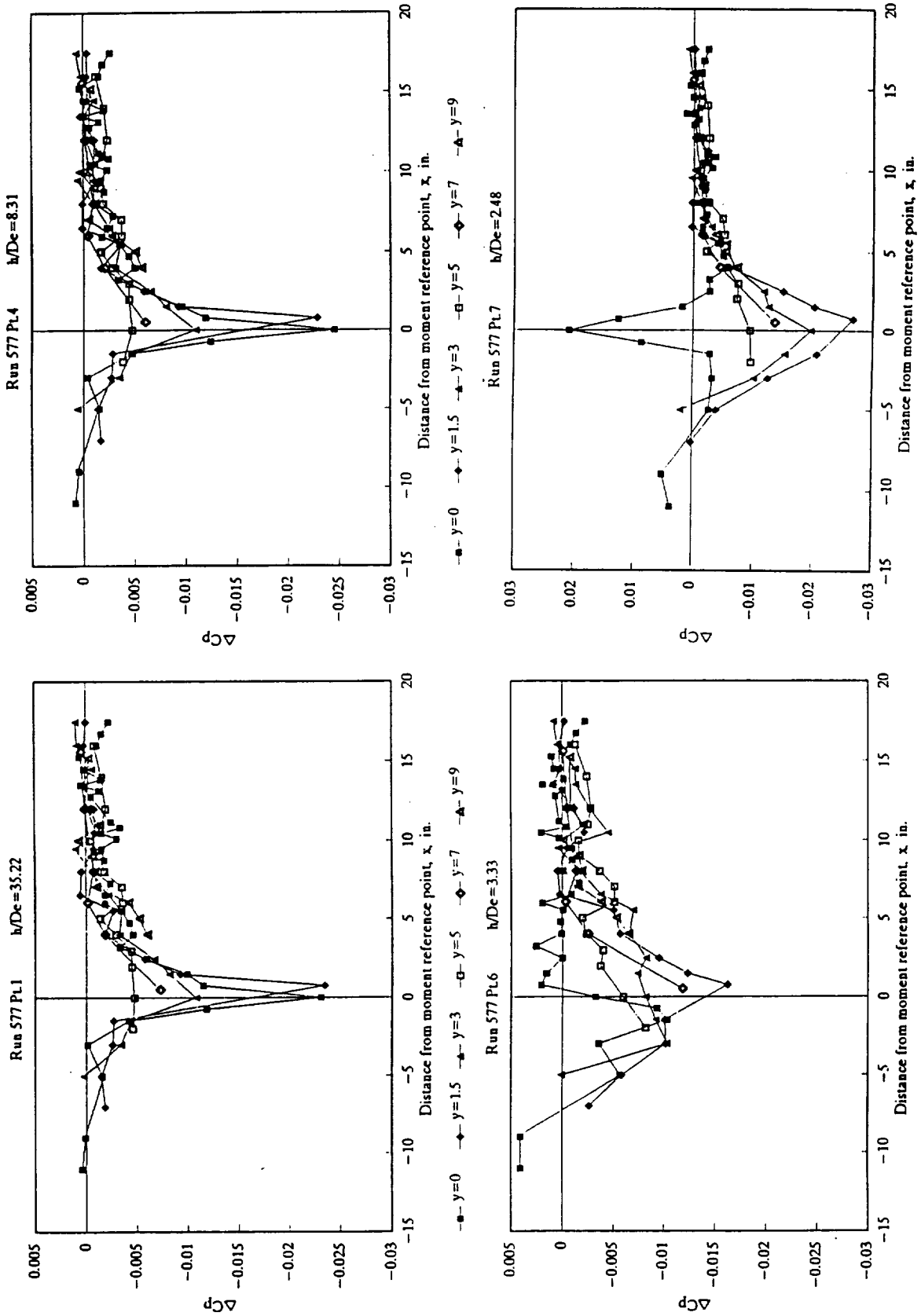
b) Out-of-Ground Effect - ref. 11 estimate.

Figure 14.- Concluded.



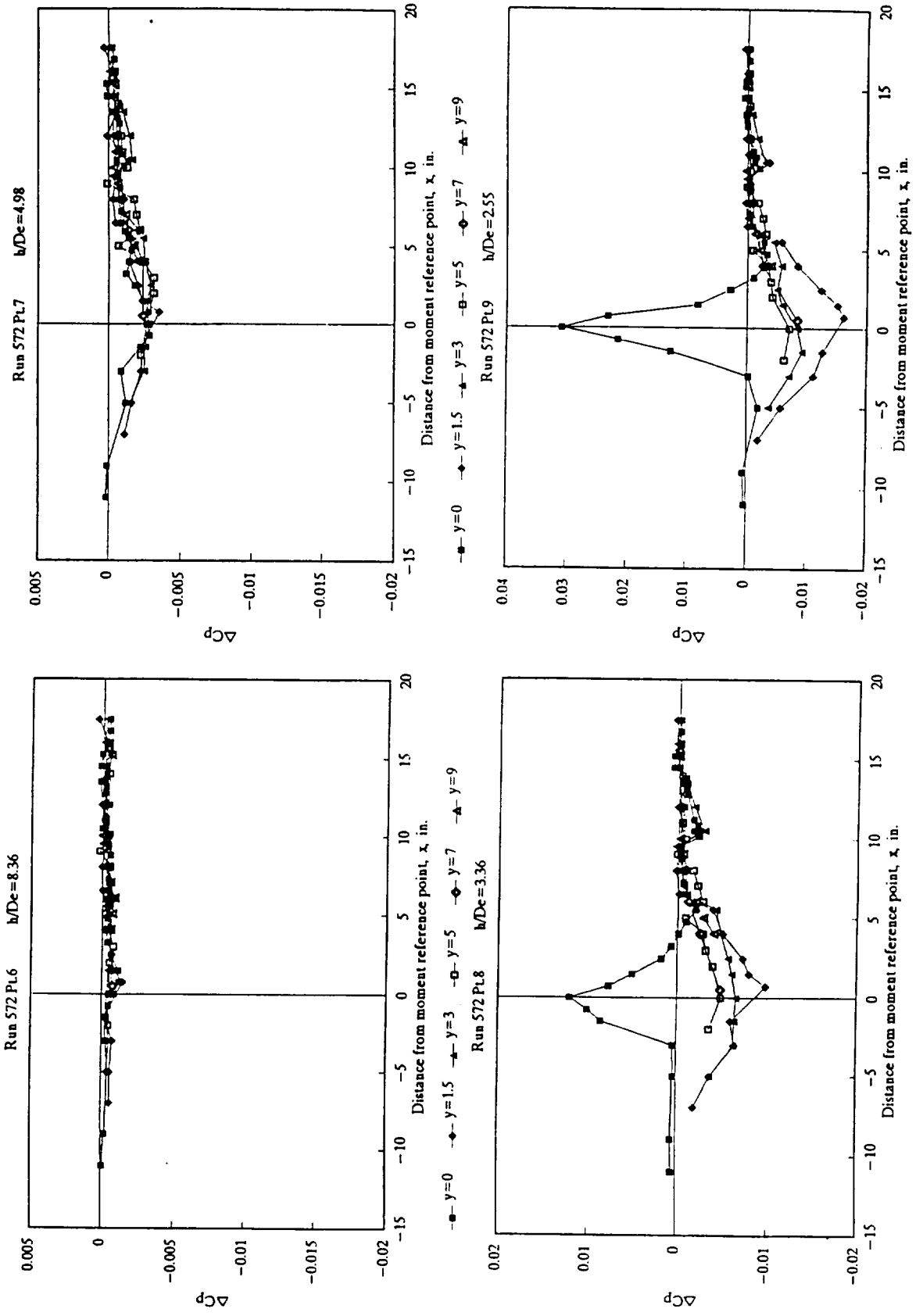
a) $V_e = .20$

Figure 15.- Chordwise distribution of jet induced pressures at selected heights - side-by-side pair at station 12.



b) $V_e = .10$

Figure 15.- Continued.



c) $V_e = 0$

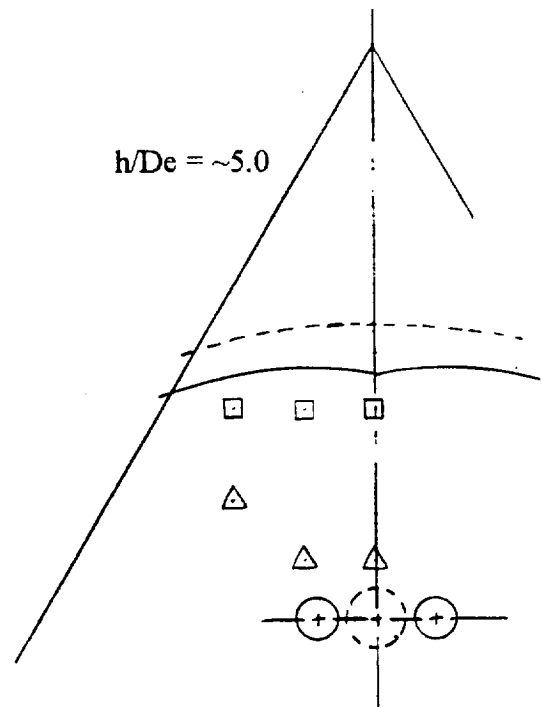
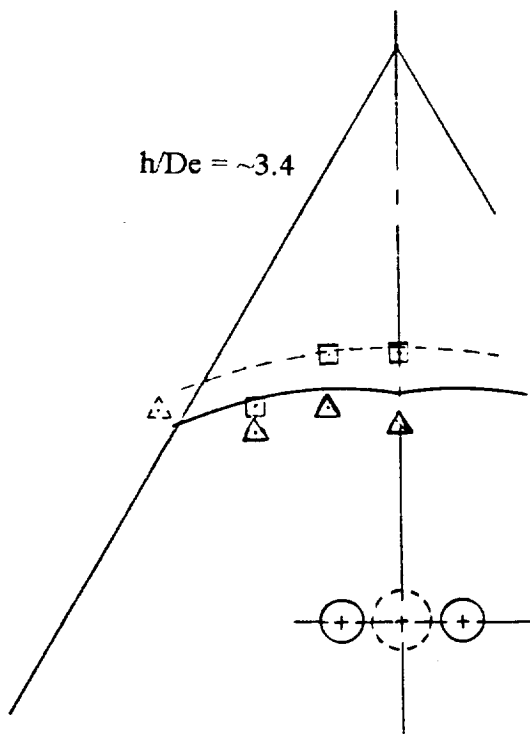
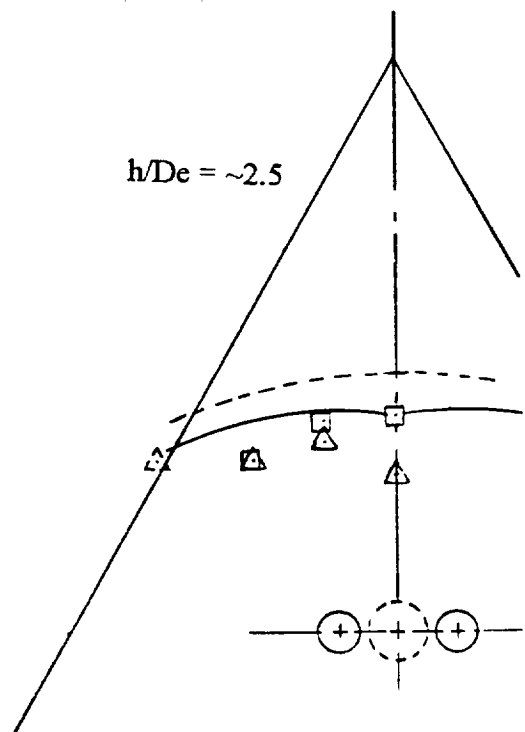
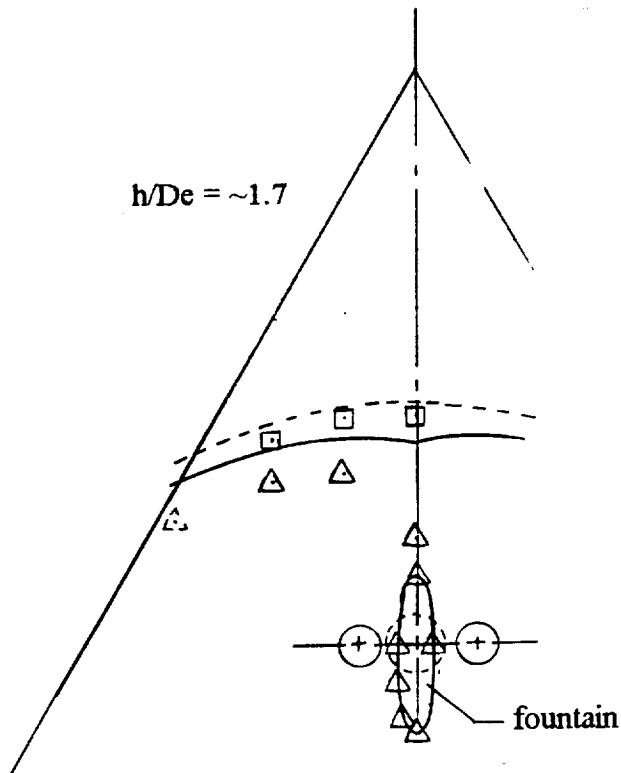
Figure 15.- Concluded.

$Ve = .2$

Estimate Data

----- □ Single Jet

————— △ Side-by-Side Pair

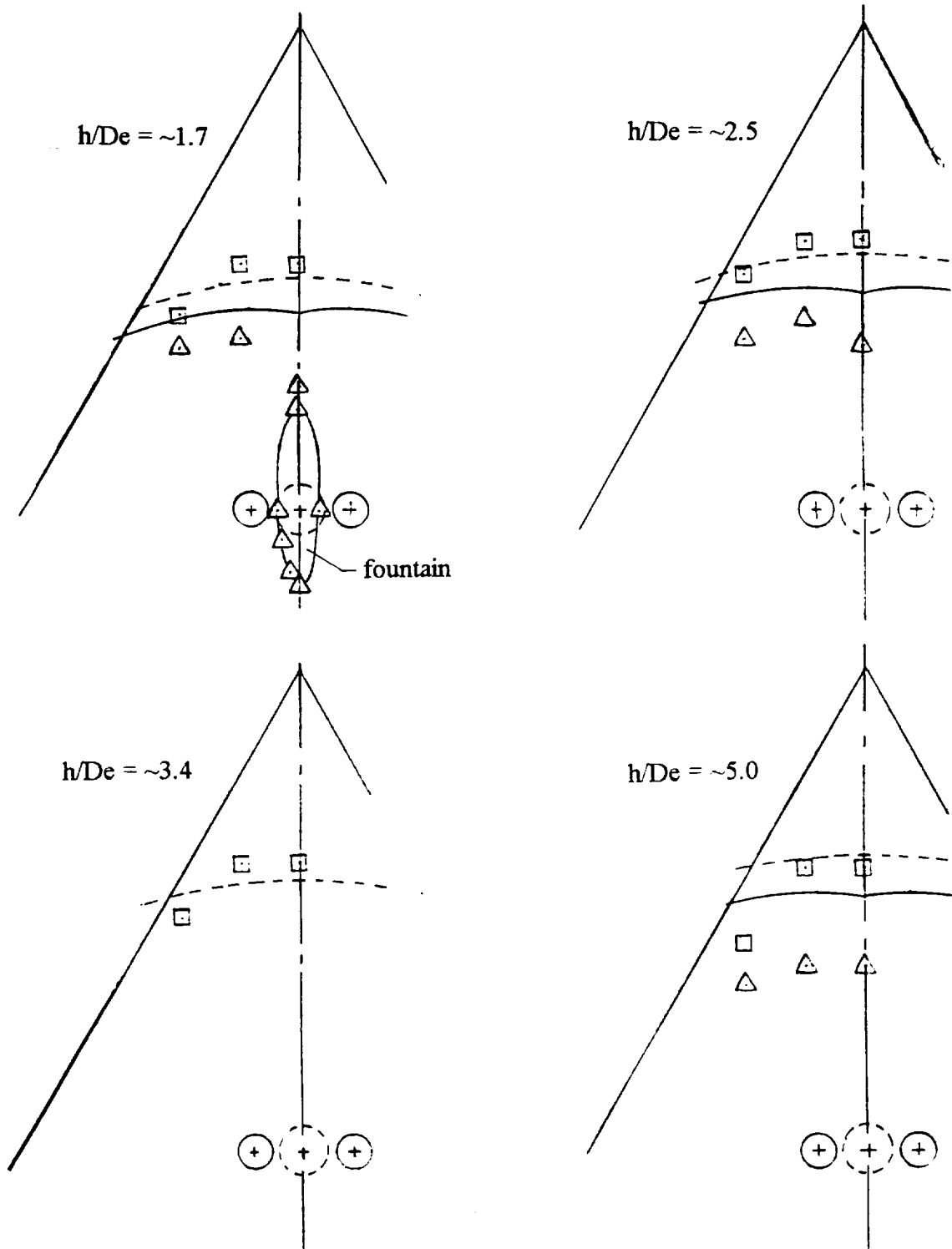


a) $Ve = .20$

Figure 16.- Comparison of location of zero pressure line for side-by-side pair with that for an equivalent single jet.

$Ve = .15$

Estimate Data
----- □ Single Jet
————— △ Side-by-Side Pair

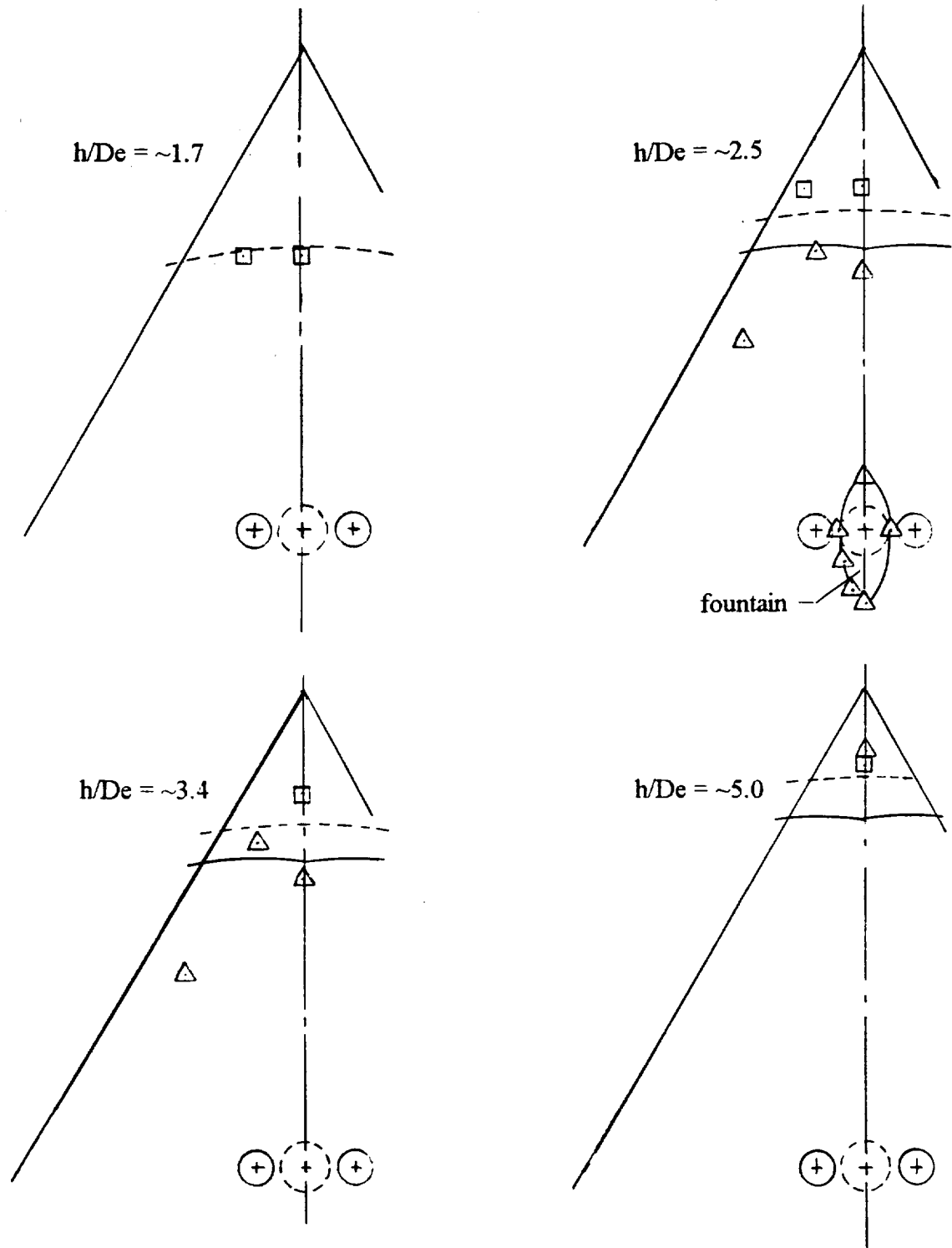


b) $v_e = .15$

Figure 16.- Continued.

$Ve = .1$

Estimate Data
----- □ Single Jet
————— △ Side-by-Side Pair



c) $Ve = .10$

Figure 16.- Concluded.

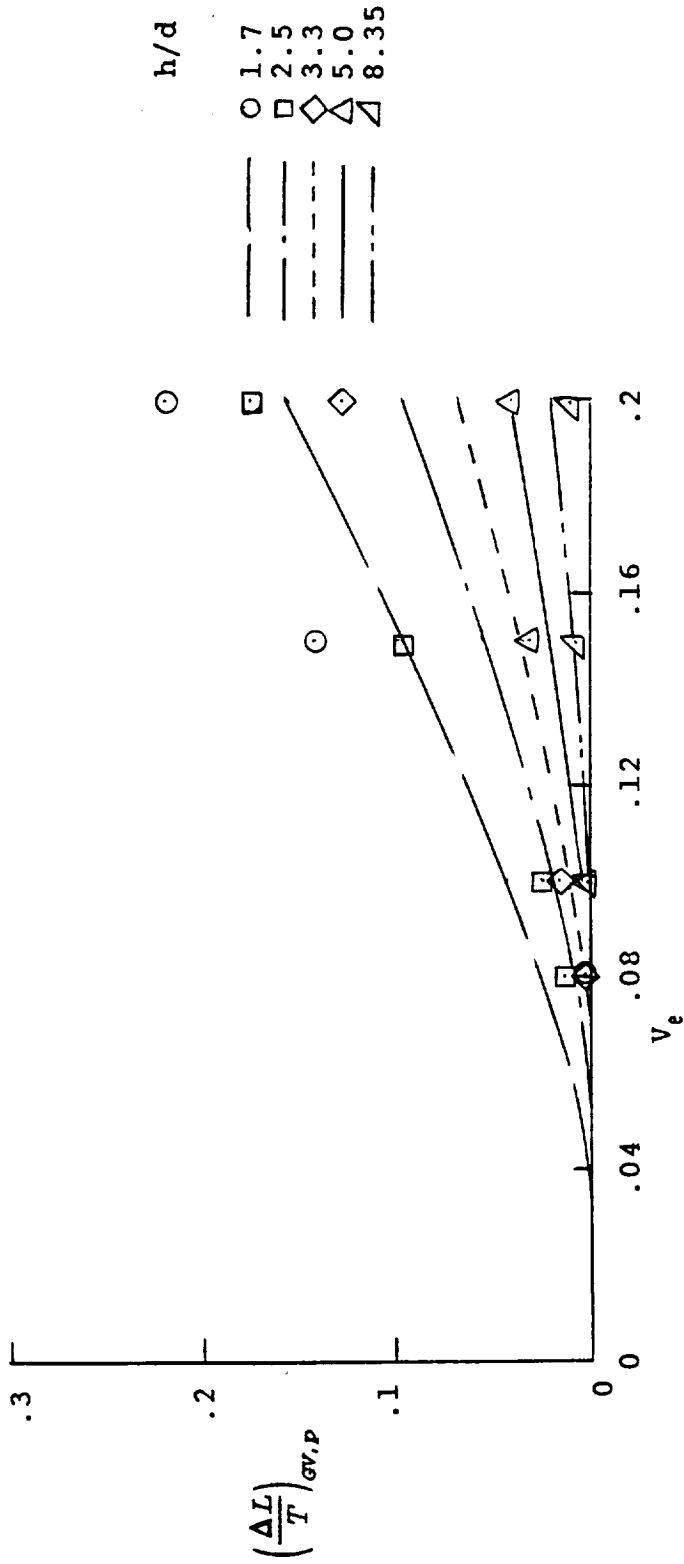


Figure 17.- Comparison of estimates of the positive lift induced by the ground vortex with the experimental data from integration of pressures forward of the zero pressure line for the side-by-side pair.

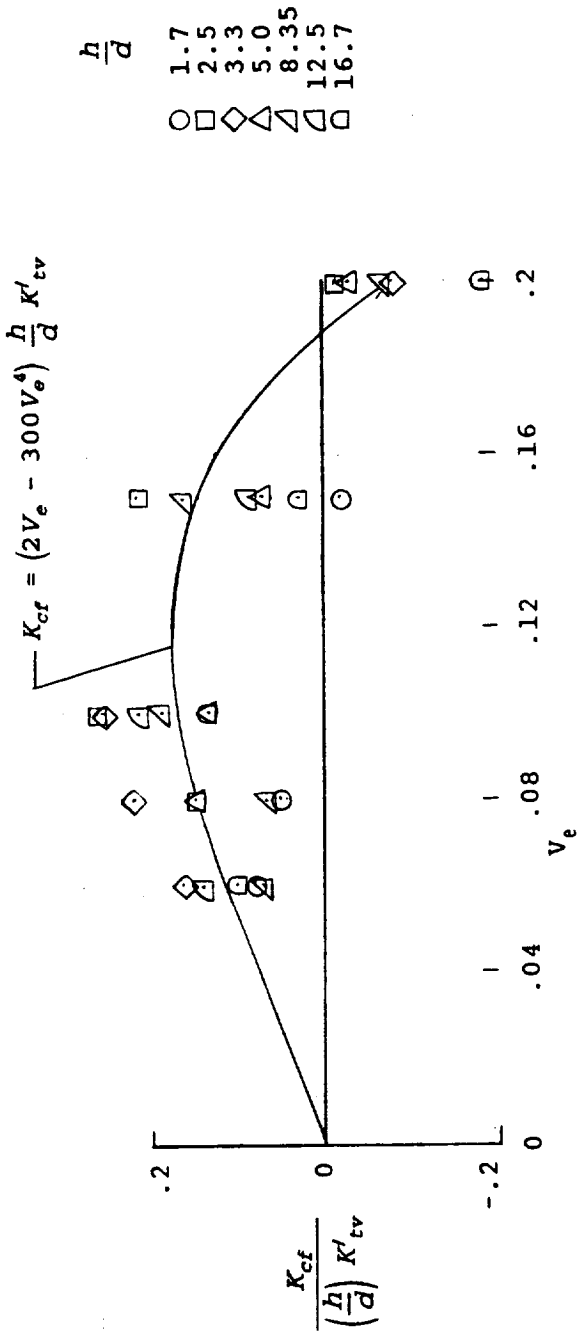


Figure 18.- Effect of height and crossflow velocity on the ratio of the crossflow lift increment to the suckdown induced in hover for the side-by-side pair.

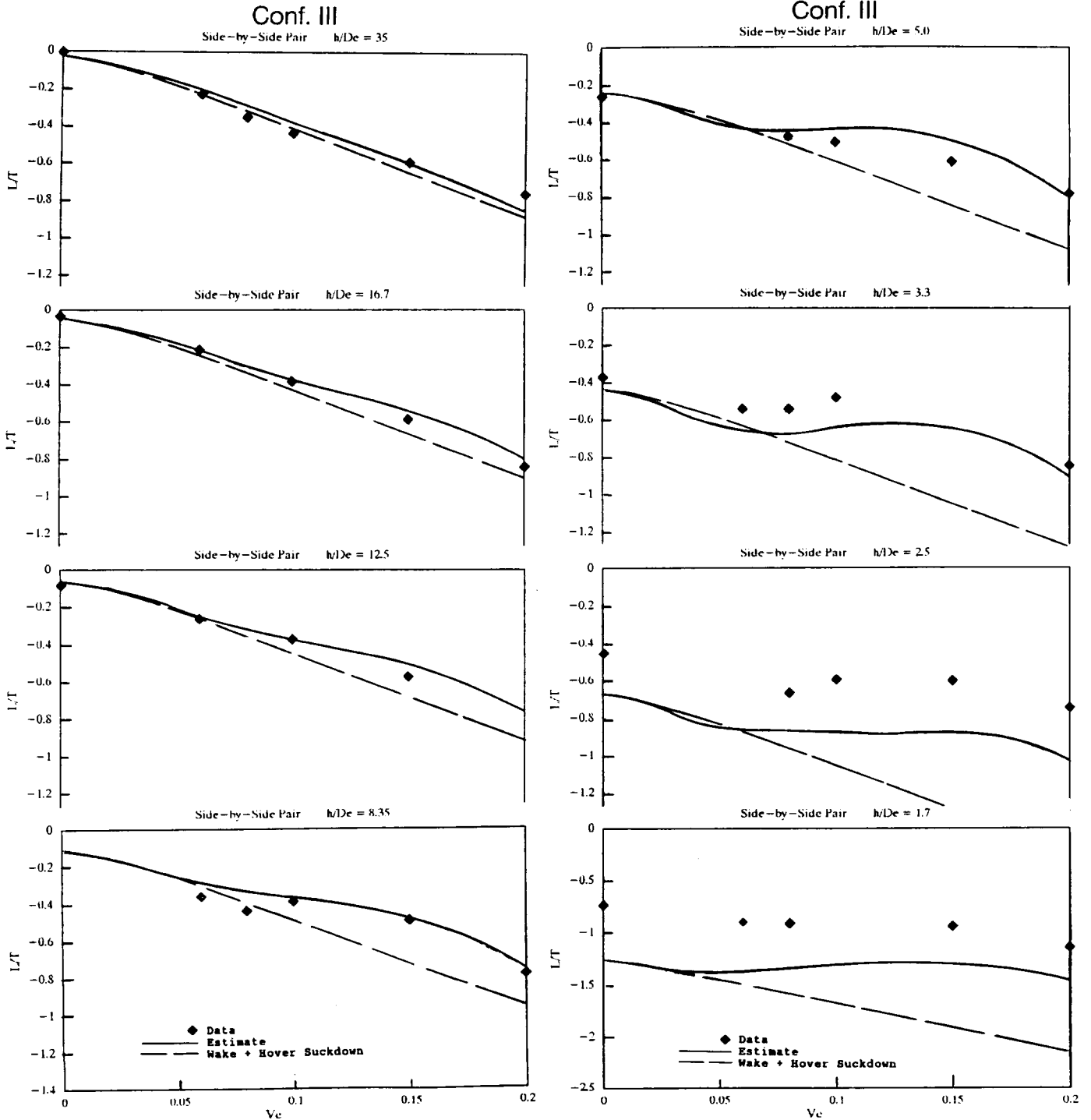
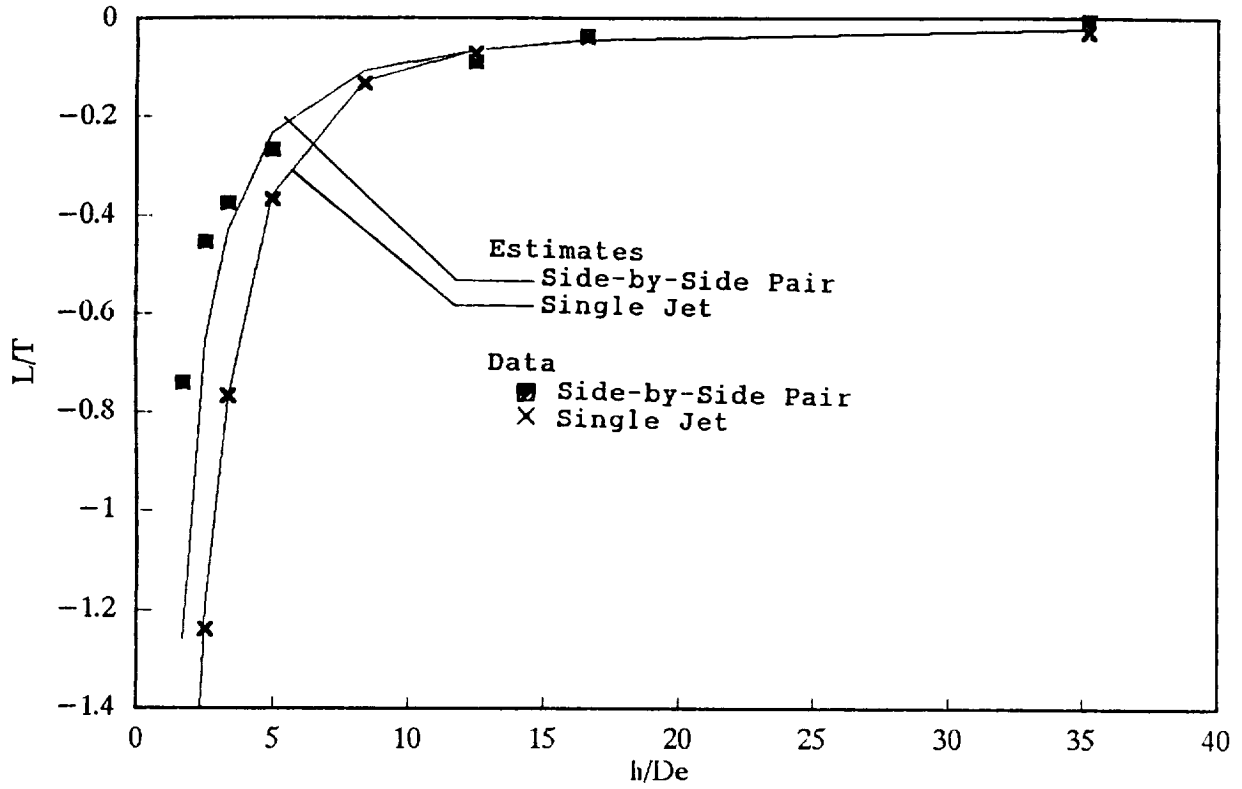


Figure 19.- Comparison of estimated net lift loss with experimental data for the side-by-side pair.

Hover Estimates



Transition – Out of Ground Effect

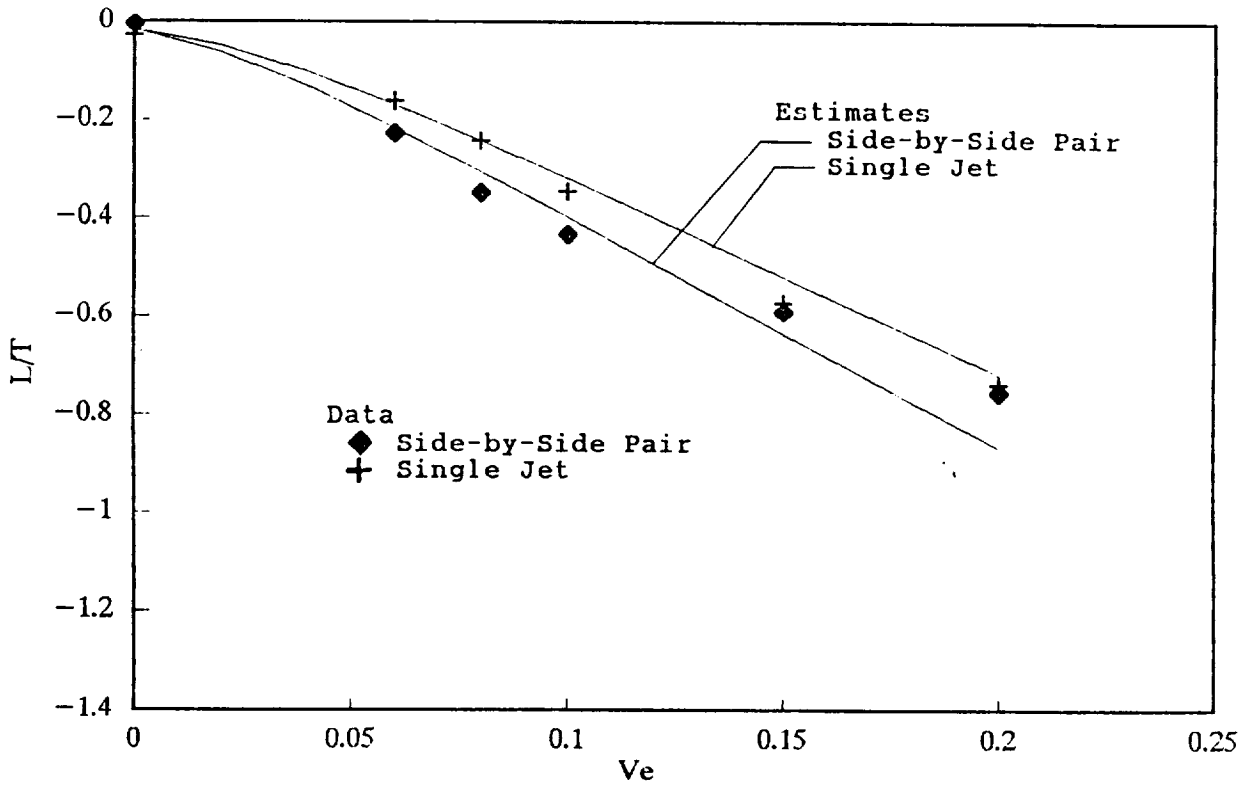


Figure 20.- Comparison of Hover and Out-of-Ground Effect estimates with data for the side-by-side pair.

REPORT DOCUMENTATION PAGE

Form Approved
OMB No. 0704-0188

Public reporting burden for this collection of information is estimated to average 1 hour per response, including the time for reviewing instructions, searching existing data sources, gathering and maintaining the data needed, and completing and reviewing the collection of information. Send comments regarding this burden estimate or any other aspect of this collection of information, including suggestions for reducing this burden, to Washington Headquarters Services, Directorate for Information Operations and Reports, 1215 Jefferson Davis Highway, Suite 1204, Arlington, VA 22202-4302, and to the Office of Management and Budget, Paperwork Reduction Project (0704-0188), Washington, DC 20503.

1. AGENCY USE ONLY (Leave blank)	2. REPORT DATE February 1998	3. REPORT TYPE AND DATES COVERED Contractor Report	
4. TITLE AND SUBTITLE The Effects of Crossflow On The Pressures and Lift Induced By The Fountain Generated Between Two Impinging Jets		5. FUNDING NUMBERS NAS2-14384; RTOP 505-68-32	
6. AUTHOR(S) Richard E. Kuhn		8. PERFORMING ORGANIZATION REPORT NUMBER A-98-09726	
7. PERFORMING ORGANIZATION NAME(S) AND ADDRESS(ES) Defense Group, Inc. 16527 Sambroso Place San Diego, CA 92128		10. SPONSORING/MONITORING AGENCY REPORT NUMBER NASA CR-206955	
9. SPONSORING/MONITORING AGENCY NAME(S) AND ADDRESS(ES) National Aeronautics and Space Administration Washington, DC 20546-0001		11. SUPPLEMENTARY NOTES Point of Contact: Doug Wardwell, Ames Research Center, MS 237-2, Moffett Field, CA 94035-1000 (650) 604-6566	
12a. DISTRIBUTION/AVAILABILITY STATEMENT Unclassified-Unlimited Subject Category - 02 Available from the NASA Center for AeroSpace Information, 800 Elkridge Landing Road, Linthicum Heights, MD 21090; (301) 621-0390.		12b. DISTRIBUTION CODE	
13. ABSTRACT (Maximum 200 words) When a jet STOVL aircraft is hovering, or in a crossflow, while close to the ground wall jets flowing radially outward from the impingement points of the jets are generated. An upflow, or fountain, is generated where the wall jets from adjacent jets meet on the ground surface. The induced lift and suckdown generated by the impingement of the fountain on the lower surface of the configuration has been the subject of previous studies. This study analyzes the limited available pressure and force data on the effect of crossflow on the fountain induced lift and suckdown. The analysis includes the effects of jet spacing, height and operating conditions. However, it is limited to twin jet configurations of circular, vertical jets operating at subcritical nozzle pressure ratios over a fixed ground surface.			
14. SUBJECT TERMS Fountain, Suckdown, STOVL		15. NUMBER OF PAGES 65	
		16. PRICE CODE A04	
17. SECURITY CLASSIFICATION OF REPORT Unclassified	18. SECURITY CLASSIFICATION OF THIS PAGE Unclassified	19. SECURITY CLASSIFICATION OF ABSTRACT	20. LIMITATION OF ABSTRACT